

Monitoring Vibrations on the Jefferson City Truss Bridge



Prepared by
Glenn Washer
Pedro Ruiz Fabian
James Dawson
Department of Civil and Environmental Engineering, University of Missouri-
Columbia



Final Report Prepared for Missouri Department of Transportation
May 2016

Project TR201605

Report cmr16-012

Technical Report Documentation Page

1. Report No. cmr 16-012	2. Government Accession No.	3. Recipient's Catalog No.	
4. Title and Subtitle Monitoring Vibrations on the Jefferson City Truss Bridge		5. Report Date Originally published: May 2016 Corrected version published: March 2017	
		6. Performing Organization Code	
7. Author(s) Glenn Washer, Pedro Ruiz Fabian, and James Dawson		8. Performing Organization Report No.	
9. Performing Organization Name and Address University of Missouri-Columbia Department of Civil and Environmental Engineering E2509 Lafferre Hall Columbia, MO 65211		10. Work Unit No. (TRAIS)	
		11. Contract or Grant No. USDOT/OST-R Grant #DTRT13-G-UTC37 and MoDOT Project #TR201605	
12. Sponsoring Organization Name and Address <div style="display: flex; justify-content: space-between;"> <div style="width: 45%;"> Midwest Transportation Center 2711 S. Loop Drive, Suite 4700 Ames, IA 50010-8664 Missouri Department of Transportation (SPR) Construction & Materials Division P.O. Box 270 Jefferson City, MO 65102 </div> <div style="width: 45%;"> U.S. Department of Transportation Office of the Assistant Secretary for Research and Technology 1200 New Jersey Avenue, SE Washington, DC 20590 </div> </div>		13. Type of Report and Period Covered Final Report (August 2015-February 2016)	
		14. Sponsoring Agency Code	
15. Supplementary Notes Visit http://www.intrans.iastate.edu/ for color pdfs of this and other research reports. MoDOT research reports are available in the Innovation Library at http://www.modot.org/services/or/byDate.htm . This report is also available at https://library.modot.mo.gov/RDT/reports/TR201605/cmr16-012.pdf .			
16. Abstract <p>The objective of the research was to determine the frequency and cause of resonant vibrations of vertical truss members on bridge A4497 over the Missouri River in Jefferson City, Missouri. Instrumentation to monitor the vibrations of four vertical members was installed on the bridge and monitored for 42 days. Weather data available from the weather station at the Jefferson City Memorial Airport were used to analyze weather conditions causing resonant vibrations of the four vertical members.</p> <p>Eleven vibration "events" were found where vertical members vibrated with higher than normal acceleration. The researchers also analyzed historical weather data to determine how frequently the resonance vibrations were occurring. The research team concluded that the frequency of resonant vibration events was likely 0.25 or fewer events per day. The vibrations were caused by average winds from the west-northwest, northwest, or southwest of approximately 17 mph or greater, based on monitoring results.</p> <p>Recommendations stemming from the research are as follows:</p> <ul style="list-style-type: none"> • The effect of the vibration events on the durability of the vertical truss members should be analyzed further to determine if a retrofit is necessary. The data provided through the field monitoring should be used in the analysis. • Other vertical members of similar lengths should be monitored to determine if they are also affected by resonant vibrations. 			
17. Key Words Data analysis; Resonance frequency; Truss bridges; Trusses; Vertical supports; Vibration; Weather conditions		18. Distribution Statement No restrictions.	
19. Security Classification (of this report) Unclassified.	20. Security Classification (of this page) Unclassified.	21. No. of Pages 64	22. Price NA

MONITORING VIBRATIONS ON THE JEFFERSON CITY TRUSS BRIDGE

**Final Report
March 2017**

Principal Investigator
Glenn Washer, Professor
Civil and Environmental Engineering, University of Missouri-Columbia

Research Assistants
Pedro Ruiz Fabian and James Dawson

Authors
Glenn Washer, Pedro Ruiz Fabian, and James Dawson

Sponsored by
Missouri Department of Transportation,
Midwest Transportation Center, and
U.S. Department of Transportation
Office of the Assistant Secretary for Research and Technology

A report from
Institute for Transportation
Iowa State University
2711 South Loop Drive, Suite 4700
Ames, IA 50010-8664
Phone: 515-294-8103 / Fax: 515-294-0467
www.intrans.iastate.edu

TABLE OF CONTENTS

ACKNOWLEDGMENTS	ix
EXECUTIVE SUMMARY	xi
1. INTRODUCTION	1
Background	1
Research Objective and Methodology	1
Vertical Truss Member Locations and Instrumentation	1
2. MONITORING SYSTEM	3
Accelerometers	3
Data Acquisition	4
Laboratory Testing.....	7
Field Implementation Testing	9
Monitoring System Installation.....	12
3. RESULTS	15
Estimated Event Rate	22
4. CONCLUSIONS.....	24
Limitations and Recommendations for Future Research.....	25
APPENDIX. GRAPHS OF DATA FROM THE VERTICAL TRUSS MEMBERS	27
A.1 Node 48	28
A.2 Node 49	34
A.3 Node 50	40
A.4 Node 51	46

LIST OF FIGURES

Figure 1. Elevation view of bridge A4497 showing the location of vertical members L21 and L21'	2
Figure 2. Microstrain G-Link sensor with power supply and enclosure attached to mounting plate	3
Figure 3. Data acquisition system integrated with essential components	4
Figure 4. Sample data collected using the SensorConnect software	6
Figure 5. System laboratory setup including a data acquisition system attached to a column (left), sensor node attached to a cabinet (middle), and sensor node attached to a movable cart (right).....	7
Figure 6. Initial (left) and final (right) timing of the first oscillation at 10 percent of the original video speed	9
Figure 7. Locations of the data acquisition system and the wireless sensors on a pedestrian truss bridge near the university for field implementation testing	10
Figure 8. Attachment of the data acquisition system (left), attachment of sensor to a tension tie (middle), and placement of sensor on the deck (right) during field implementation test.....	10
Figure 9. Impact on a tension tie via rubber mallet (left) and impact on the deck by jumping (right) during field implementation testing	11
Figure 10. Data collected for Node 48 during field implementation testing	11
Figure 11. Installation of the data acquisition system on vertical member L22	12
Figure 12. Location of sensor nodes mounted on verticals L21 and L21'	13
Figure 13. Installation of wireless sensor nodes	14
Figure 14. Typical acceleration data from a vertical member showing two “events”	16
Figure 15. Cardinal wind directions.....	21
Figure 16. Correlation between maximum winds and maximum accelerations	22
Figure 17. Data collected for Node 48 from January 27 to February 1, 2016.....	28
Figure 18. Data collected for Node 48 from February 1 to February 10, 2016.....	29
Figure 19. Data collected for Node 48 from February 10 to February 15, 2016.....	30
Figure 20. Data collected for Node 48 from February 29 to March 7, 2016.....	31
Figure 21. Data collected for Node 48 from March 7 to March 14, 2016.....	32
Figure 22. Data collected for Node 48 from March 14 to March 22, 2016.....	33
Figure 23. Data collected for Node 49 from January 27 to February 1, 2016.....	34
Figure 24. Data collected for Node 49 from February 1 to February 10, 2016.....	35
Figure 25. Data collected for Node 49 from February 10 to February 15, 2016.....	36
Figure 26. Data collected for Node 49 from February 29 to March 7, 2016.....	37
Figure 27. Data collected for Node 49 from March 7 to March 14, 2016.....	38
Figure 28. Data collected for Node 49 from March 14 to March 22, 2016.....	39
Figure 29. Data collected for Node 50 from January 27 to February 1, 2016.....	40
Figure 30. Data collected for Node 50 from February 1 to February 10, 2016.....	41
Figure 31. Data collected for Node 50 from February 10 to February 15, 2016.....	42
Figure 32. Data collected for Node 50 from February 29 to March 7, 2016.....	43
Figure 33. Data collected for Node 50 from March 7 to March 14, 2016.....	44
Figure 34. Data collected for Node 50 from March 14 to March 22, 2016.....	45
Figure 35. Data collected for Node 51 from January 27 to February 1, 2016.....	46

Figure 36. Data collected for Node 51 from February 1 to February 10, 2016	47
Figure 37. Data collected for Node 51 from February 10 to February 15, 2016	48
Figure 38. Data collected for Node 51 from February 29 to March 7, 2016	49
Figure 39. Data collected for Node 51 from March 7 to March 14, 2016	50
Figure 40. Data collected for Node 51 from March 14 to March 22, 2016	51

LIST OF TABLES

Table 1. Location information for equipment installed on bridge A4497	13
Table 2. Occurrence times for events identified during the monitoring period.....	17
Table 3. Node peak accelerations for each individual event	18
Table 4. Resonating frequency of the nodes for each event	19
Table 5. Recorded wind speed and direction for each event	19
Table 6. Cardinal wind directions based on degrees of of direction.....	20
Table 7. Average wind speed, standard deviation, and 95 percent confidence level wind speed based on event data collected during field-testing.....	22
Table 8. Average wind direction, standard deviation, and 95 percent confidence level wind direction based on the events collected during field-testing	23

ACKNOWLEDGMENTS

This project was funded by the Missouri Department of Transportation, the Midwest Transportation Center, and the U.S. Department of Transportation Office of the Assistant Secretary for Research and Technology.

EXECUTIVE SUMMARY

The objective of this research was to determine the frequency and cause of resonant vibrations of truss vertical members on bridge A4497 over the Missouri River in Jefferson City, Missouri. Instrumentation to monitor the vibrations of four vertical members was installed on the bridge and monitored for 42 days. The instrumentation included four wireless accelerometers, which were used to monitor the vertical members' resonant vibration accelerations.

Weather data available from the weather station located at the Jefferson City Memorial Airport were used to analyze the weather conditions that caused the resonant vibrations of the vertical members during field monitoring. Eleven vibration "events" were found where the vertical members vibrated with higher than normal acceleration. The average wind speed during the events was about 17 mph. The wind direction during the events was from the west-northwest or northwest during nine of the events and from the southeast during two of the events. The researchers found that the frequency of the events was 0.26 events per day during the monitoring period.

The researchers also analyzed historical weather data for a previous 446-day period to determine how frequently the resonance vibrations were occurring (i.e., how frequently the combined wind speed and direction matched the conditions determined through field monitoring). The research team found there were 89 occurrences of the combined wind speeds and directions that could cause vibrations of the vertical truss members. The resulting frequency of events was determined to be 0.20 events per day.

The researchers concluded that the frequency of resonant vibration events was likely 0.25 or fewer events per day. The vibrations were caused by average winds from the west-northwest, northwest, or southwest of approximately 17 mph or greater, based on monitoring results. Recommendations stemming from the research are as follows:

- The effect of the vibration events on the durability of the vertical members should be analyzed further to determine if a retrofit is necessary. The data provided through the field monitoring should be used in the analysis.
- Other vertical members of similar lengths should be monitored to determine if they are also affected by resonant vibrations.

1. INTRODUCTION

Background

The Jefferson City Bridge is the name for two continuous arch truss bridges over the Missouri River in Jefferson City, Missouri. US 54 crosses the river between Callaway County, Missouri on the north and Cole County, Missouri on the south over these two bridges. This report documents research conducted to study resonant vibrations occurring on vertical truss members of bridge A4497, which is the north(east)bound bridge that was built in 1991.

Vibration of the vertical members was observed on several occasions by Missouri Department of Transportation (MoDOT) staff working in the area. The vibration of the vertical members was observed during periods of relatively high winds. It was not known how frequently the resonant vibrations were occurring. The actual wind speed and direction that excited resonance vibrations in the vertical members was not well defined.

Research Objective and Methodology

The objective of this research was to determine the frequency and cause of the observed resonant vibrations of bridge A4497's vertical truss members.

Instrumentation to monitor the vibrations of four vertical members, on each side of the center of the two trusses on either side of the bridge, was installed and monitored for 42 days. Weather data available from the weather station at the Jefferson City Memorial Airport were used to analyze the area weather conditions causing resonant vibrations of the vertical members. The researchers analyzed the data to determine how frequently resonant vibrations were occurring and to determine the ambient weather conditions (i.e., wind speeds and directions) that caused the vibrations.

Based on these data, the researchers also analyzed historical weather data over a period of 446 days to determine how frequently the resonant vibrations were occurring (i.e., how frequently the combined wind speeds and directions matched the conditions determined through the field monitoring).

Vertical Truss Member Locations and Instrumentation

The two vertical member sets that were monitored as part of the study were L21 and L21', circled in Figure 1.

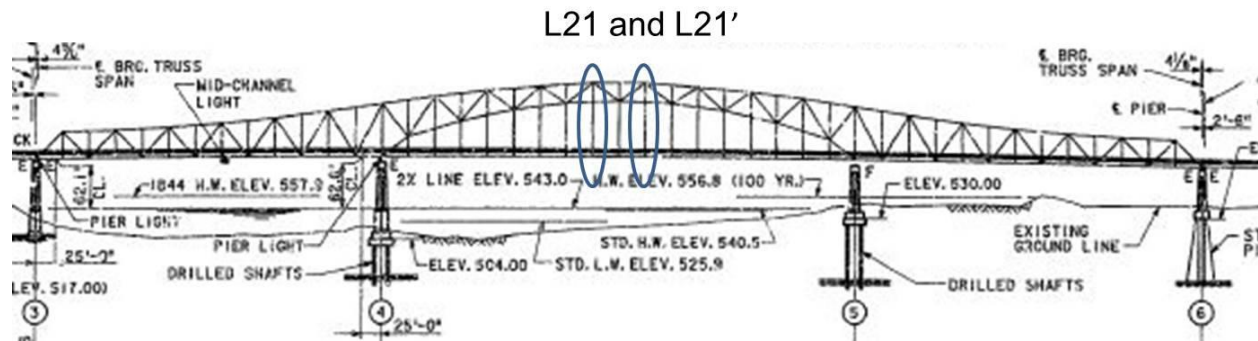


Figure 1. Elevation view of bridge A4497 showing the location of vertical members L21 and L21'

The two L21 members are on the south side of the truss centerline and the two L21' members are on the north side of the truss centerline. Each I-shaped vertical member is comprised of two steel flanges (0.75 x 12 in.) and a web plate (0.375 x 19.5 in.)

Instrumentation comprised of wireless accelerometers were installed on each vertical member to monitor vibrations. The next chapter describes the laboratory and field implementation testing undertaken prior to installing the accelerometers on the bridge.

2. MONITORING SYSTEM

This chapter describes the field monitoring system developed to monitor the vibrations of four truss vertical members. A hard-wired monitoring system, where each sensor was connected directly to a central data acquisition system, was not practical. Therefore, wireless sensors were used.

Accelerometers

Four wireless Microstrain G-Link sensor nodes were used to monitor vibrations of the vertical members. The Microstrain G-Link sensor is a battery-operated high-speed tri-axial accelerometer with user-programmable sampling rates of up to 4,096 Hz. These sensors are capable of measuring accelerations of up to 10 G (with 1 G being equal to the acceleration from gravity). Figure 2 shows one of the sensor nodes.

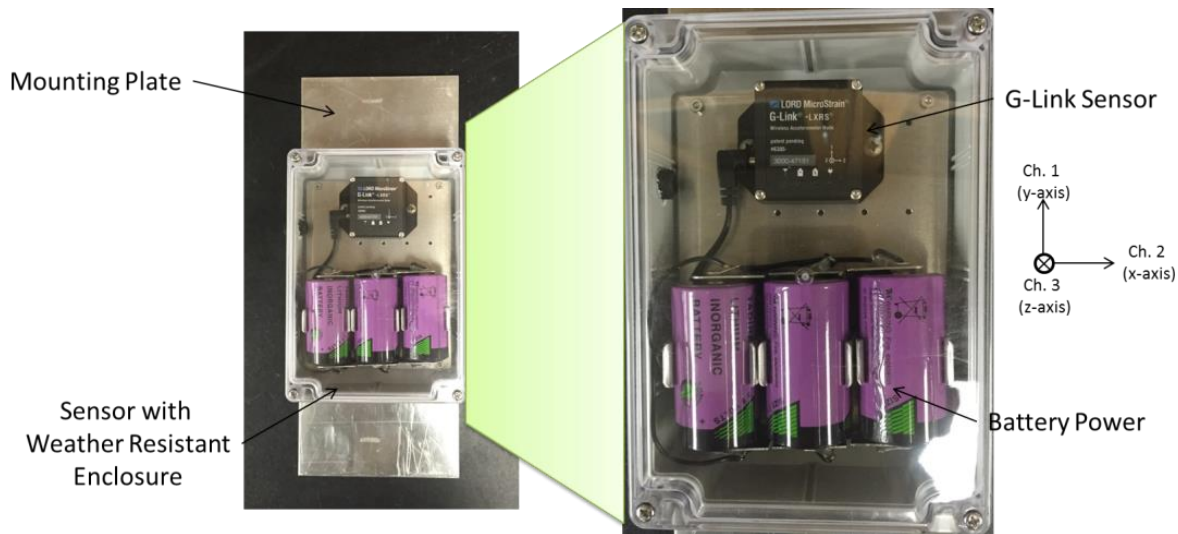


Figure 2. Microstrain G-Link sensor with power supply and enclosure attached to mounting plate

The sensor and supporting batteries were mounted in a weather-resistant enclosure. In order to attach the enclosure to the flanges of the vertical members, an aluminum mounting plate was fabricated and attached to the back of the enclosure. The mounting plate with the sensor enclosure was attached to the flanges of the vertical member using small flange clamps. In this orientation, the y-axis of the accelerometer was aligned vertically with the member so vibrations resulting from member resonance would not be expected on the vertical axis of the sensor (Channel 1). The x-axis and z-axis of the accelerometer were aligned to detect flexural and torsional vibrations of the member, respectively. The four wireless sensor nodes were identified as Node 48, Node 49, Node 50, and Node 51.

Data Acquisition

Figure 3 shows the data acquisition system used in this research: a Dell notebook, Microstrain USB base station, and Cisco router, all enclosed in a fiberglass enclosure, with conduit out of the enclosure for the connection to the power supply.

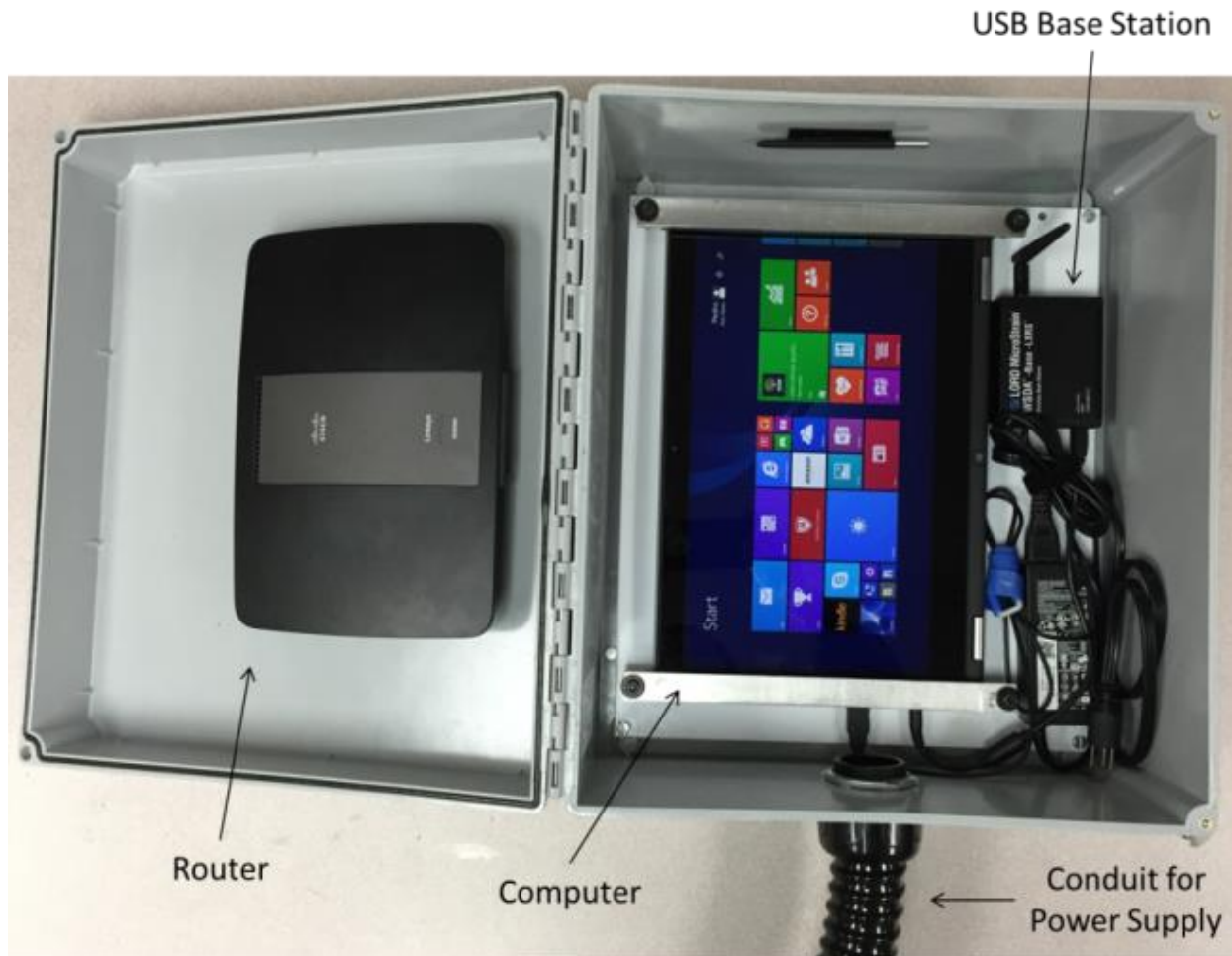


Figure 3. Data acquisition system integrated with essential components

The data acquisition enclosure was used to protect the base station and computer from the elements. The notebook and USB base station were both attached to a mounting plate via screws, and the mounting plate was attached to the fiberglass enclosure. The router was attached to the enclosure using Velcro strips. The notebook computer was used to run the software necessary for the wireless sensor nodes to communicate with the Microstrain USB base station and to store the data received from the sensors. The router was used for wireless communication with the computer for the purpose of downloading data. An Ethernet connection was also used to download the data. The system was powered by alternating current (AC) power, provided on-site.

The software package SensorConnect (beta version) was used for this research due to its ability to record and read the large data files collected during testing. Figure 4 shows the SensorConnect display screen with the USB base station and the nodes collecting data. The nodes were programmed to sample at a continuous rate of 16 Hz based on laboratory testing and video analysis.

Node 47148

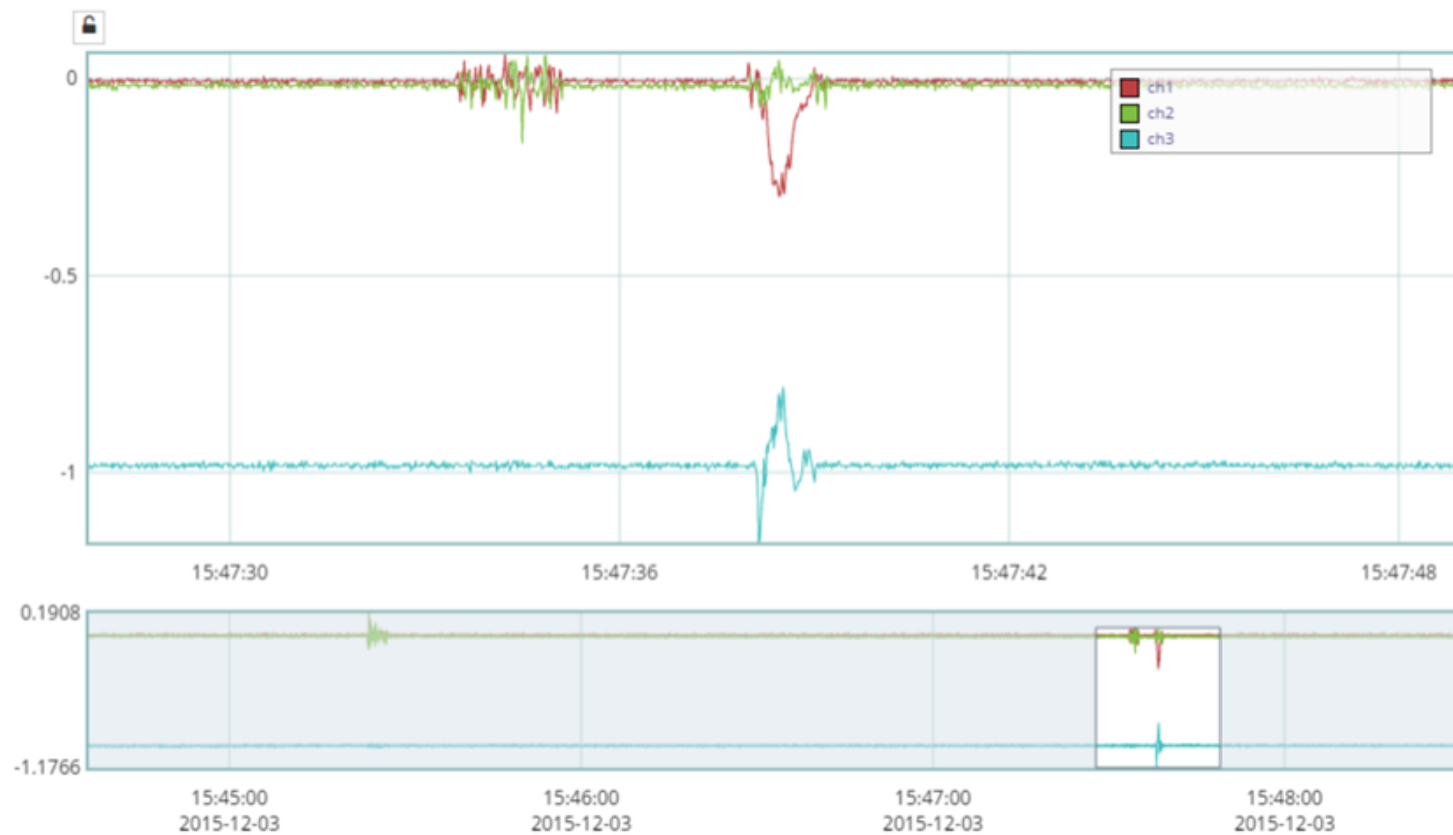


Figure 4. Sample data collected using the SensorConnect software

The SensorConnect software records data continuously and stores the data in computer memory. The data can then be retrieved through the attached router or Ethernet connection while the sensors continue to collect data. To post-process the data, the downloaded files were inserted into the SensorConnect program on a separate computer, which was manually analyzed to identify data of interest (i.e., periods where the vertical members were undergoing large amplitude vibrations). These data were exported for post-processing using both Microsoft Excel and the Mathworks Matlab programs.

Laboratory Testing

The monitoring system was tested in the laboratory to ensure proper operation. Testing was geared towards troubleshooting the data collection system and ensuring that data were being successfully collected and downloaded. Figure 5 illustrates the system in a laboratory-based setup.



Figure 5. System laboratory setup including a data acquisition system attached to a column (left), sensor node attached to a cabinet (middle), and sensor node attached to a movable cart (right)

The data acquisition system was attached to a column to simulate the system's attachment in the field, and the sensor nodes were mounted to various objects in the laboratory, such as a cabinet and movable cart. Data were collected over a period of several weeks and downloaded periodically to simulate the anticipated field conditions. These tests were used to ensure that the software was operating reliably, data could be downloaded without interruption to system operation, and estimates could be developed for the time required to download datasets of different sizes.

During the laboratory testing, the research team found that the system's standard software was inadequate for downloading datasets of the size required for field monitoring. Working with the manufacturer, a beta version of an updated version of the software was acquired to support the field-testing. This beta version supported downloading and analyzing datasets of the size anticipated for this bridge monitoring project.

Based on the amount of time required to download the data collected over a period of several weeks, it was determined that the wireless router was too slow to be practically implemented in the field. Therefore, a wired Ethernet connection was used for the field-testing. The Ethernet connection was also successfully tested in the laboratory to collect and download data over a time period of several weeks.

Required Data Acquisition Rates

The digital data acquisition of accelerometer data required continuous, periodic, or threshold-based collection. Periodic data collection is appropriate for health monitoring applications in which accelerations may vary over long time intervals. Monitoring the accelerations of a bridge for one hour each week in order to detect changes in acceleration resulting from deterioration of bridge members is an example of periodic data collection.

Threshold-based data collection means that data is only recorded to memory when defined threshold amplitudes of the acceleration are exceeded. Threshold-based data collection is appropriate when anticipated acceleration amplitudes are known either from previous experience or from analysis.

For bridge A4497, the anticipated acceleration amplitudes resulting from the vibration of the members were not known. Consequently, continuous monitoring of the data was chosen as the approach for the research. However, continuous monitoring of the acceleration data results in very large datasets that can be difficult to manage. Therefore, it was necessary to limit the data sampling rate to the greatest extent possible to limit the size of the resulting datasets.

The data sampling rate is the number of data points stored to the computer memory per second. Generally, data sampling rates of at least twice the frequency of vibration are necessary to reproduce the frequency and amplitude of a signal that is captured digitally. To determine the minimum data sampling rate to be used to monitor vibrations of bridge A4497, a video of a vibrating vertical member was analyzed.

The frequency of the vibration was determined by slowing down the video to 10 percent of its original speed using the software package Final Cut Pro. The timing of a single oscillation was determined at the reduced speed and then converted back to the original video speed. Figure 6 shows the initial timing of the beginning of the oscillation and the final timing at the end of the oscillation, with the video rotated 90 degrees. Once the time change was determined, the time was converted back to the original video time speed to calculate the frequency of vibration.

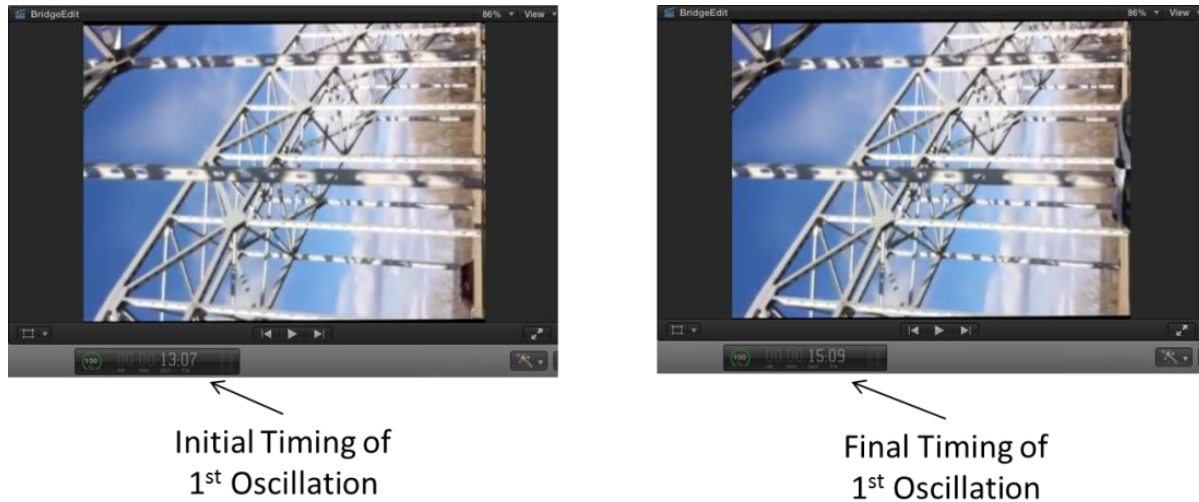


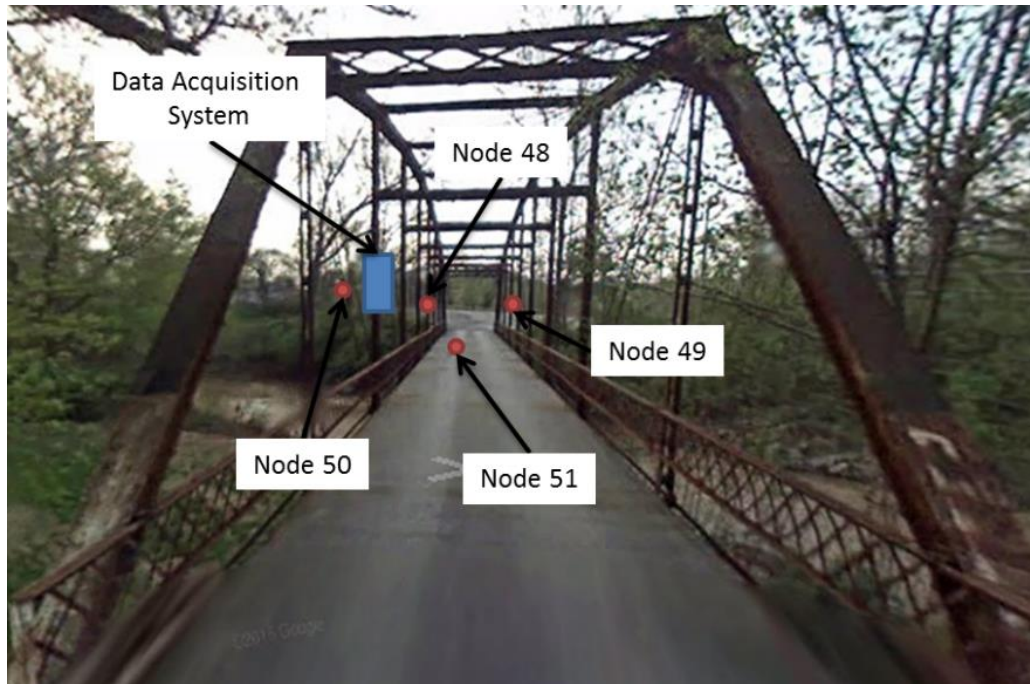
Figure 6. Initial (left) and final (right) timing of the first oscillation at 10 percent of the original video speed

As shown in Figure 6, the change in time for a single oscillation was determined to be 0.203 s. The frequency was then calculated to be 4.84 Hz for a single cycle of vibration. A similar analysis was completed for five cycles of oscillations using the video at reduced speed. The time necessary for five oscillations was determined to be 9.90 s. Based on these data, the researchers concluded that the members were oscillating at a frequency of about 5 Hz. Therefore, a data sampling rate of at least 10 Hz would be necessary to capture the frequency content of the vibrations.

Based on these data, a sampling rate of 16 Hz was used in the field. To ensure that this sampling rate would produce accurate results, data from a field implementation test were analyzed, as described in the next section.

Field Implementation Testing

A field implementation test of the monitoring system was performed to ensure that all components of the system would perform adequately in the field and to practice field installation. The data acquisition system was installed on a vertical member of a pedestrian truss bridge located near the University of Missouri-Columbia. During the test, Nodes 48, 49, and 50 were attached to diagonal tension ties, and Node 51 was placed on the deck of the bridge. Figure 7 shows the locations of the data acquisition system and the wireless sensor nodes.



©2015 Google Streetview

Figure 7. Locations of the data acquisition system and the wireless sensors on a pedestrian truss bridge near the university for field implementation testing

The sensor nodes were mounted on tension ties that were observed to be carrying different amounts of tensile load based on their vibrations following an impact on the tie. Different amounts of tension in the diagonal ties produced different frequencies when impacted. This allowed for a variety of different vibration frequencies to be tested. Figure 8 shows the attachment of the data acquisition system to a vertical member and sensor node placement on a tension tie and on the bridge deck.



Figure 8. Attachment of the data acquisition system (left), attachment of sensor to a tension tie (middle), and placement of sensor on the deck (right) during field implementation test

Testing of the sensors was completed by initiating the data acquisition software with a defined sampling rate of 4, 8, or 16 Hz. The diagonal tension tie was then impacted twice using a rubber mallet near each of the sensor nodes. The sensor node located on the bridge deck was excited by

jumping on the bridge deck. Figure 9 shows the impacts on a tension tie with a rubber mallet and a jump near the sensor on the deck of the bridge.



Figure 9. Impact on a tension tie via rubber mallet (left) and impact on the deck by jumping (right) during field implementation testing

Figure 10 shows the results of the impacts near Node 48, with different sampling rates used for each set of impacts.

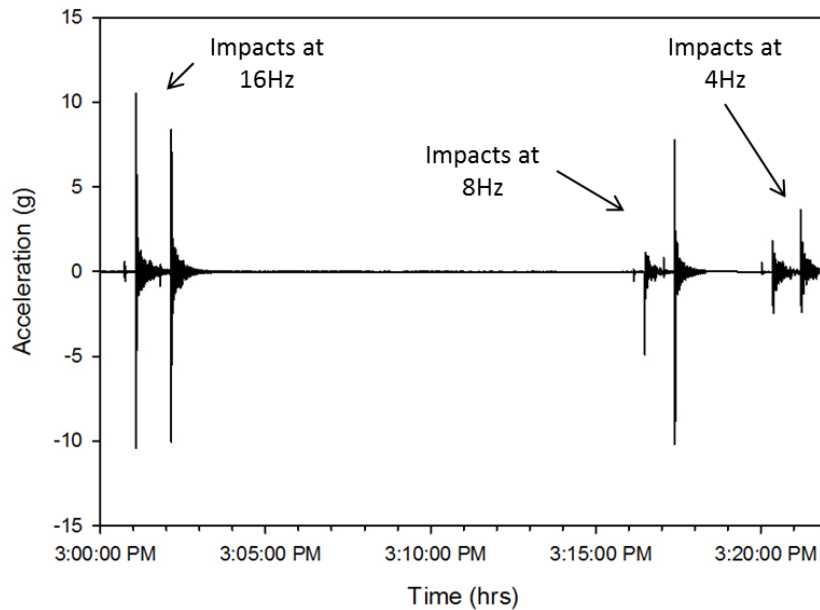


Figure 10. Data collected for Node 48 during field implementation testing

The data were assembled from different tests to illustrate the effect of the different sampling rates. The effect of different data acquisition rates were clearly observed in the different impact sets. As shown in Figure 10, the amplitude of the impacts could not be properly reproduced in

the digital data when acquisition rates of less than 16 Hz were used. This effect was caused by the under sampling of data (i.e., the data sampling rate not being sufficiently high). Sampling rates of greater than 16 Hz were not considered due to practical limitations. Specifically, datasets would be too large to be efficiently downloaded in the field. Because the sampling rate of 16 Hz was three times the frequency calculated through the video analysis and exceeded the minimum sampling rate of 10 Hz, it was determined to be adequate to meet the objectives of the research. Using the sampling rate of 16 Hz, seven days of data collection from the four accelerometers produced two gigabytes of data.

Monitoring System Installation

The installation of the field monitoring system on bridge A4497 was successfully completed with the aid of MoDOT staff on Wednesday, January 27, 2016. Installation began by closing down the right driving lane of the bridge to allow for the installation of the AC power necessary for the monitoring system to operate. Once the power was installed, the data acquisition system was installed about 10 ft up on vertical member L22, located on the bridge's east side. Figure 11 shows the data acquisition system installed on L22.



Figure 11. Installation of the data acquisition system on vertical member L22

After the installation of the data acquisition system, the system was tested and data were downloaded to ensure that all sensor nodes were working properly and communicating with the base station. Installation of two of the wireless sensors (Node 48 and Node 49) followed.

Figure 12 shows the locations of the nodes on bridge A4497 in schematic diagrams with both the elevation view of the bridge (top) and the locations of the sensor nodes on the vertical members (bottom).

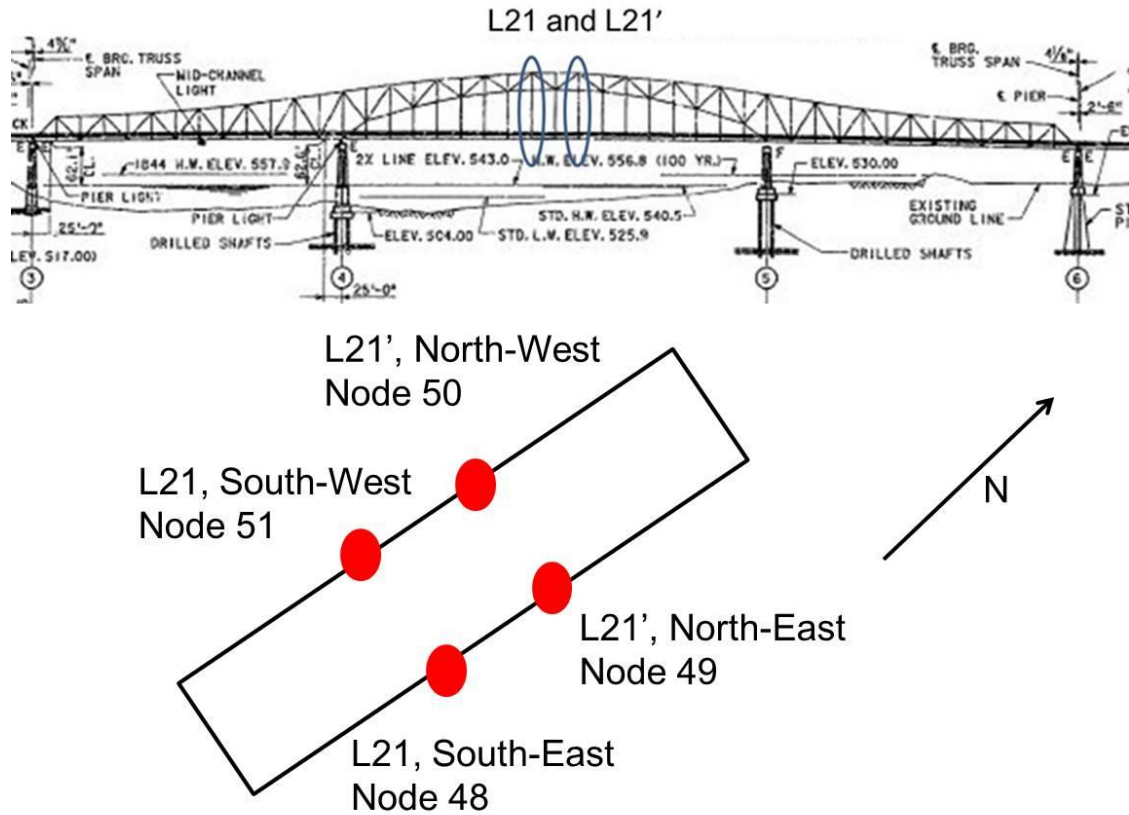


Figure 12. Location of sensor nodes mounted on verticals L21 and L21'

Node 48 was installed on vertical member L21 on the southeast side of the bridge, while Node 51 was installed on vertical member L21 on the southwest side of the bridge. Node 49 was installed on vertical member L21' on the northeast side of the bridge, while Node 50 was installed on vertical member L21' on the northwest side of the bridge.

Table 1 includes a summary of the location information for sensor nodes mounted on bridge A4497.

Table 1. Location information for equipment installed on bridge A4497

Equipment	Member	Location
Data Acquisition System	L22	East side
Node 48	L21	Southeast side
Node 49	L21'	Northeast side
Node 50	L21'	Northwest side
Node 51	L21	Southwest side

Figure 13 shows one of the wireless sensor nodes being installed. All four of the wireless sensors were installed about 30 ft above the roadway.

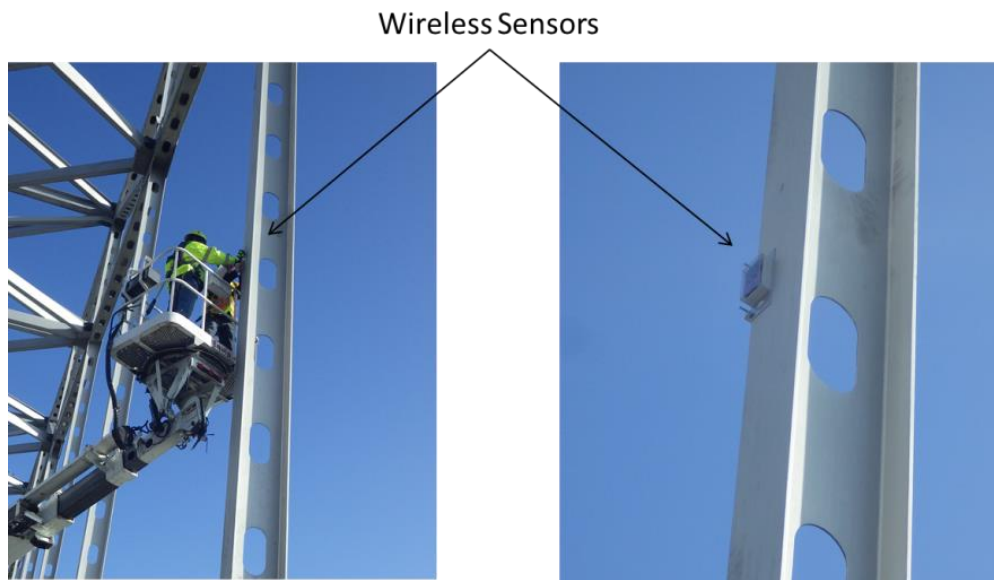


Figure 13. Installation of wireless sensor nodes

3. RESULTS

Testing of bridge A4497 began on January 27, 2016 and continued through February 15, 2016. At that time, testing stopped due to a loss of communication between the wireless sensor nodes and the data acquisition system. The cause of this loss of communication was not known and could not be reproduced in the laboratory.

The computer used for data acquisition was replaced in an effort to stop any future loss of communication. The system was restarted on February 29, 2016 and data were collected until the system was removed on March 22, 2016. The system was removed at that time for two reasons. First, the monitoring system indicated that communication with the sensor nodes had been lost. It was later realized that communication had not been lost, and data were still being collected even though the system indicated data collection was not occurring. Second, the system needed to be removed prior to the start of a maintenance project that would limit the ability to support necessary lane closures on the bridge. In total, data were collected for 42 days.

Data collected during this time period were analyzed to identify when resonance vibrations were occurring on the bridge. The nominal vibrations occurring on the four vertical members during normal traffic loading was analyzed, and it was determined that the nominal vibrations were generally 0.25 G or less. Based on these data, a resonance “event” was identified as a vibration amplitude of greater than 0.25 G for an extended period of time, typically more than one hour. Figure 14 shows typical data collected on a vertical truss member.

As shown in the figure, events were identified from the peak amplitudes of vibrations. During the 42 days of testing, 11 different “events” were identified in the data. As shown in Figure 14, vibration amplitudes varied during a typical “event” and were grouped together to form an individual “event.”

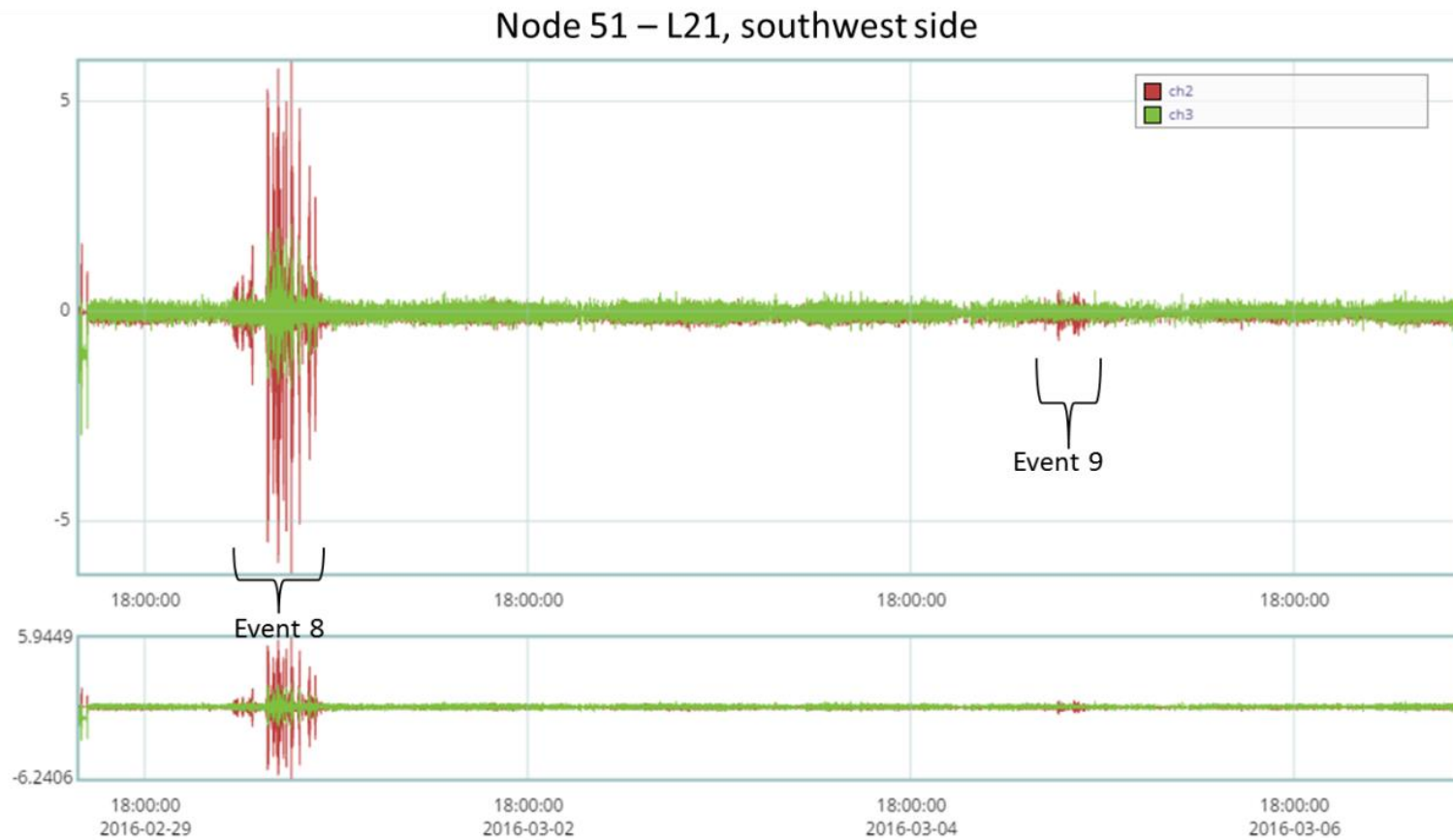


Figure 14. Typical acceleration data from a vertical member showing two “events”

Table 2 shows all 11 events that occurred during the monitoring period, along with their start and end dates and times and duration (in hours).

Table 2. Occurrence times for events identified during the monitoring period

Event	Start Date	End Date	Start Time	End Time	Duration (hrs.)
#1	1/28/2016	1/28/2016	1:00 p.m.	5:30 p.m.	4.5
#2	1/31/2016	1/31/2016	12:30 p.m.	2:00 p.m.	1.5
#3	2/2/2016	2/2/2016	5:30 a.m.	8:00 a.m.	2.0
#4	2/3/2016	2/3/2016	10:00 a.m.	2:30 p.m.	4.5
#5	2/7/2016	2/9/2016	10:00 p.m.	7:00 p.m.	45.0
#6	2/12/2016	2/12/2016	11:00 a.m.	3:00 p.m.	4.0
#7	2/13/2016	2/14/2016	11:30 p.m.	6:30 a.m.	7.0
#8	3/1/2016	3/1/2016	5:00 a.m.	4:30 p.m.	11.5
#9	3/5/2016	3/5/2016	12:00 p.m.	4:00 p.m.	4.0
#10	3/15/2016	3/15/2016	5:00 p.m.	9:00 p.m.	4.0
#11	3/19/2016	3/19/2016	11:00 a.m.	2:00 p.m.	3.0

As shown in Table 2, the “events” typically occurred during the daytime, between the hours of 5:00 a.m. and 9:00 p.m. One of the events lasted for several days. The duration of the events ranged from a low of 1.5 hrs. to a maximum of 45 hrs. As noted previously, the - vibrations varied during the course of an individual event, such that the high-amplitude vibrations were not continuous throughout the 45-hour time period. Graphs of the data for all of the events identified during the monitoring period are included in the Appendix.

As shown previously in Figure 14, data were collected only for Channels 2 and 3 of the tri-axial node sensors, on the x-axis and z-axis, respectively, as described previously. The peak accelerations for Channels 2 and 3 of each individual node for each event are shown in Table 3.

Table 3. Node peak accelerations for each individual event

Event	Peak Acceleration (G)							
	Node 48		Node 49		Node 50		Node 51	
	Chan. 2	Chan. 3	Chan. 2	Chan. 3	Chan. 2	Chan. 3	Chan. 2	Chan. 3
#1	0.45	0.3	0.46	0.24	0.52	0.29	0.56	0.36
#2	0.49	0.29	0.44	0.16	0.31	0.28	0.39	0.27
#3	1.42	0.35	1.23	0.29	0.44	0.27	1.28	0.48
#4	1.84	0.69	1.70	0.63	3.09	1.13	5.82	1.96
#5	2.93	1.05	1.92	0.69	4.20	1.46	7.10	2.44
#6	0.62	0.33	0.54	0.26	0.99	0.39	3.20	1.09
#7	1.75	0.70	0.70	0.26	0.82	0.35	3.73	1.38
#8	2.03	1.15	1.34	0.52	2.45	0.96	5.94	2.08
#9	0.43	1.00	0.46	0.17	0.48	0.27	0.52	0.46
#10	0.66	0.96	0.66	0.23	0.59	0.31	0.83	0.42
#11	0.68	0.52	0.53	0.17	0.44	0.19	0.95	0.37
Avg.	1.21	0.67	0.91	0.33	1.30	0.54	2.76	1.03

These peak accelerations were determined by finding the highest acceleration experienced during an individual event. The greatest peak lateral accelerations occurred on Node 51 (L21, southwest) with an acceleration of 7.10 G, while the greatest peak torsional acceleration also occurred on the same node with an acceleration of 2.44 G. Overall, Node 51 exhibited the highest peak acceleration, both laterally and torsional for all of the events analyzed. The second highest overall peak lateral acceleration occurred on Node 50 (L21', northwest), while the second highest overall peak torsional acceleration occurred on Node 48 (L21, southeast).

The researchers also conducted a frequency analysis on the data collected for each event. The purpose of the frequency analysis was to determine the frequency at which the vertical truss members were resonating and to confirm the video analysis. The data for each individual event were analyzed with a fast Fourier transform (FFT) using the MatLab program. The results of this analysis determined the frequency of the resonating vertical members. Table 4 details the frequency that each node was resonating during each event.

Table 4. Resonating frequency of the nodes for each event

Event	Frequency (Hz)							
	Node 48		Node 49		Node 50		Node 51	
	Chan. 2	Chan. 3	Chan. 2	Chan. 3	Chan. 2	Chan. 3	Chan. 2	Chan. 3
#1	5.32	5.32	5.30	5.30	5.23	5.23	5.24	5.23
#2	5.31	5.31	5.28	5.28	5.23	5.23	5.23	5.23
#3	5.32	5.32	5.30	5.30	5.24	5.24	5.24	5.24
#4	5.31	5.31	5.29	5.29	5.22	5.22	5.23	5.23
#5	5.31	5.31	5.29	5.29	5.22	5.22	5.23	5.23
#6	5.32	5.32	5.30	5.30	5.23	5.23	5.23	5.23
#7	5.32	5.32	5.30	5.30	5.24	5.24	5.24	5.24
#8	5.30	5.30	5.29	5.29	5.22	5.22	5.23	5.23
#9	5.31	5.31	5.29	5.29	5.23	5.23	5.24	5.24
#10	5.30	5.30	5.28	5.28	5.21	5.21	5.22	5.22
#11	5.31	5.31	5.29	5.29	5.23	5.23	5.23	5.23
Avg.	5.31	5.31	5.29	5.29	5.23	5.23	5.23	5.23

The highest frequency of 5.32 Hz occurred on Node 48 and the lowest frequency of 5.21 Hz occurred on Node 50. Table 4 shows that the average overall frequency was 5.27 Hz. The average frequency was 8.8 percent higher than the original calculated frequency of 4.84 Hz from the video analysis. Generally, the research found little variation in the vibration frequencies determined for the different vertical members and events.

Table 5 details the wind speed and direction for each event that occurred during field-testing on the bridge.

Table 5. Recorded wind speed and direction for each event

Event	Wind Speed (mph)			Wind Direction (degrees)		
	Low	High	Average	Low	High	Average
#1	15.0	20.7	17.3	300.0	320.0	308.0
#2	13.8	20.7	17.3	300.0	310.0	305.0
#3	16.1	21.9	19.0	110.0	120.0	115.0
#4	13.8	23.0	18.6	280.0	310.0	294.3
#5	11.5	29.9	17.4	280.0	320.0	306.0
#6	11.5	19.6	15.5	290.0	350.0	307.1
#7	12.7	18.4	15.1	110.0	140.0	123.3
#8	6.9	24.2	16.9	260.0	320.0	301.3
#9	10.4	17.3	14.3	300.0	320.0	310.0
#10	15.0	31.1	23.7	270.0	300.0	290.0
#11	12.7	18.4	15.6	280.0	320.0	300.0

The average wind speeds and directions in Table 5 show the average of the conditions during the duration of each event. The high and low values during each event are also shown. The wind conditions were tracked using the wind readings at the nearest weather station, at the Jefferson City Memorial Airport. The researchers tracked the data online at www.weatherunderground.com.

Wind speeds reported by the weather service are based on wind speed averages for two-minute durations. For every hour, the researchers selected a two-minute time period in which wind speed measurements were recorded every five seconds. The average of these measurements was then designated as the “average” wind speed for that hour. The lowest average wind velocity that was observed during an event was 14.3 mph, while the highest observed was 23.7 mph. The wind directions were recorded in degrees.

Table 6 and Figure 15 show the correlation between cardinal direction assigned and wind direction in degrees.

Table 6. Cardinal wind directions based on degrees of direction

Cardinal Direction	Degree Direction
N	348.75–11.25
NNE	11.25–33.75
NE	33.75–56.25
ENE	56.25–78.75
E	78.75–101.25
ESE	101.25–123.75
SE	123.75–146.25
SSE	146.25–168.75
S	168.75–191.25
SSW	191.25–213.75
SW	213.75–236.25
WSW	236.25–258.75
W	258.75–281.25
WNW	281.25–303.75
NW	303.75–326.25
NNW	326.25–348.75

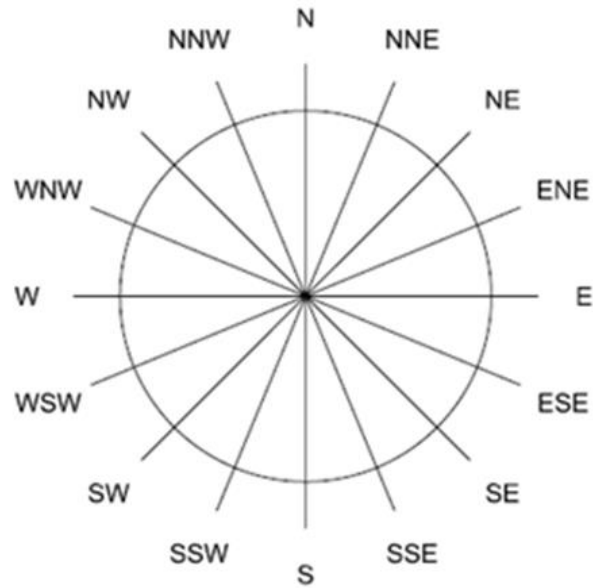


Figure 15. Cardinal wind directions

From the previous Table 5, two events occurred with average wind directions ranging between 115.0° to 123.3° (i.e., with winds coming out of the east-southeast). The remaining nine events had an average wind direction ranging from 290.0° to 310.0° (i.e., with winds coming out of the west-northwest or northwest).

Figure 16 shows the correlation between the maximum winds recorded for each event and the maximum acceleration measured by each sensor node.

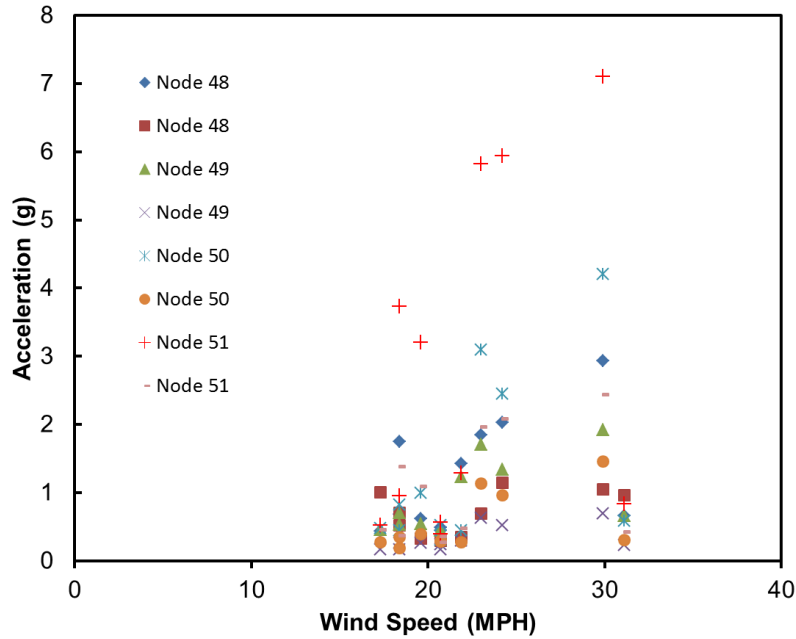


Figure 16. Correlation between maximum winds and maximum accelerations

As shown, Node 51 typically exhibited much higher accelerations than other sensor nodes; Node 50 also exhibited higher accelerations than the other sensor nodes. These sensor nodes were located on vertical truss members L21 and L21' on the west side of bridge A4497.

Estimated Event Rate

The field monitoring and data analysis described previously provided the characteristic wind speeds and directions that caused resonant vibrations in the vertical members. The monitoring provided a limited sampling period of 42 days during which 11 events occurred. To extend the analysis and determine how frequently the events were occurring over the course of a year or more, the researchers analyzed historical weather data from the Jefferson City Memorial Airport weather station to determine the rate at which the events were occurring.

The average speed for winds coming from the west-northwest or northwest and those from the southeast are shown in Table 7.

Table 7. Average wind speed, standard deviation, and 95 percent confidence level wind speed based on event data collected during field-testing

	Wind Speed (mph)	
	WNW/NW	SE
Average	17.4	17.0
σ	2.7	2.8
-2σ	12.0	11.5

The average speed for winds from the west-northwest or northwest was 17.4 mph with a standard deviation (σ) of 2.7 mph, while the average speed for winds from the southeast was 17.0 mph with a standard deviation of 2.8 mph. Table 8 shows that the average wind direction for the nine events coming from the west-northwest or northwest was of 302.4° with a standard deviation of 6.7° , while the average wind direction for the two events from the southeast was 119.2° with a standard deviation of 5.9° .

Table 8. Average wind direction, standard deviation, and 95 percent confidence level wind direction based on the events collected during field-testing

	Wind Direction (degrees)	
	WNW/NW	SE
Average	302.4	119.2
σ	6.7	5.9
-2σ	289	107
2σ	316	131

Average and standard deviations were used for both wind speed and wind direction analyses using historical data. Weather data were obtained for 446 days from January 1, 2015 through March 21, 2016. These data were analyzed through Microsoft Excel using the averages obtained from the events recorded during field monitoring. It was assumed that these data were normally distributed so that using \pm two standard deviations would capture all events with a confidence that exceeded 95 percent. The values for this can be seen in Table 7 and Table 8 for the wind speeds and wind directions, respectively. For the wind speed, only the -2σ was used given that this was a minimum threshold.

The researchers analyzed the historical weather data by determining the number of hours in which the combined wind speed and direction occurred during the 446 days. The researchers then divided this number of hours by the average time period for events, as determined from the field testing.

Using these parameters and the average duration of the events for winds coming from the west-northwest or northwest and southeast, the team determined 56 events would have come from the west-northwest or northwest, while 33 would have come from the southeast. That is a total of 89 events exhibiting weather conditions resulting in the resonance phenomenon during the 446-day period when weather data were analyzed. This is a rate of 0.20 events per day, or one event every five days.

From the field monitoring, 11 events were recorded in 42 days for a rate of 0.26 events per day, or about one event every four days. So, the rates determined from the field monitoring and analysis of historical weather data were similar.

4. CONCLUSIONS

The objective of this research was to determine the frequency and cause of resonant vibrations of truss vertical members on bridge A4497 over the Missouri River in Jefferson City, Missouri. Data from field monitoring were used to identify both when resonant vibrations were occurring and the wind speed and direction at the time of the vibrations. Historical weather data were also analyzed to determine how frequently the defined wind speed and direction combination occurred over a period of 446 days. From these data, the rate of occurrence of the resonant vibrations was determined.

The researchers concluded that the frequency of resonant vibration events was likely 0.25 or fewer events per day. The vibrations were caused by average winds from the west-northwest or northwest or southwest of approximately 17 mph or greater, based on monitoring results.

Specific conclusions from the field monitoring data are as follows:

- For a total of 42 days, data were collected with 11 events occurring at a rate of 0.26 events per day during the field-testing time period.
- The average wind direction for nine of the events was from the west-northwest or northwest, with the two remaining events coming from the southeast.
- Average wind speed from the west-northwest or northwest was 17.4 mph, ranging from 14.3 mph to 23.7 mph during each event.
- Average wind speed from the southeast was 17.0 mph, ranging from 15.1 mph to 19.0 mph during each event.
- The lowest maximum wind speed to result in an event was 17.3 mph.

Specific conclusions from the historical weather data analysis are as follows:

- 446 days of data were collected, with 89 events occurring at a rate of 0.20 events per day during the time period in which data were analyzed.
- Ultimately, 56 events were found with winds coming from the west-northwest or northwest, with the remaining 33 events with winds coming from the southeast.
- A difference of only 0.06 events per day or 23.1 percent was found between the results of the data collected during field testing and the historical data.

Limitations and Recommendations for Future Research

The research determined the characteristic weather conditions and frequency of resonant vibrations of the four vertical members. However, the research did not attempt to analyze the effect of these vibrations on the durability of the bridge members. The research led to the following recommendations:

- The effect of the vibration events on the durability of the members should be analyzed further to determine if a retrofit is necessary. The data provided through the field monitoring should be used in the analysis. Additional monitoring should be considered if a retrofit is installed.
- Other vertical members of a similar length should be monitored to determine if they are affected by resonant vibrations. The members that were monitored were selected based on observed vibrations; other truss members may be similarly affected, perhaps with lower magnitude vibrations that are not so easily observed visually.

APPENDIX. GRAPHS OF DATA FROM THE VERTICAL TRUSS MEMBERS

This appendix includes graphs of all of the data collected using the four accelerometers during the field-testing period. The graphs are organized by node, each of which was located on an individual vertical truss member. For the location of each node, see Figure 12 and Table 1 in Chapter 2.

A.1 Node 48

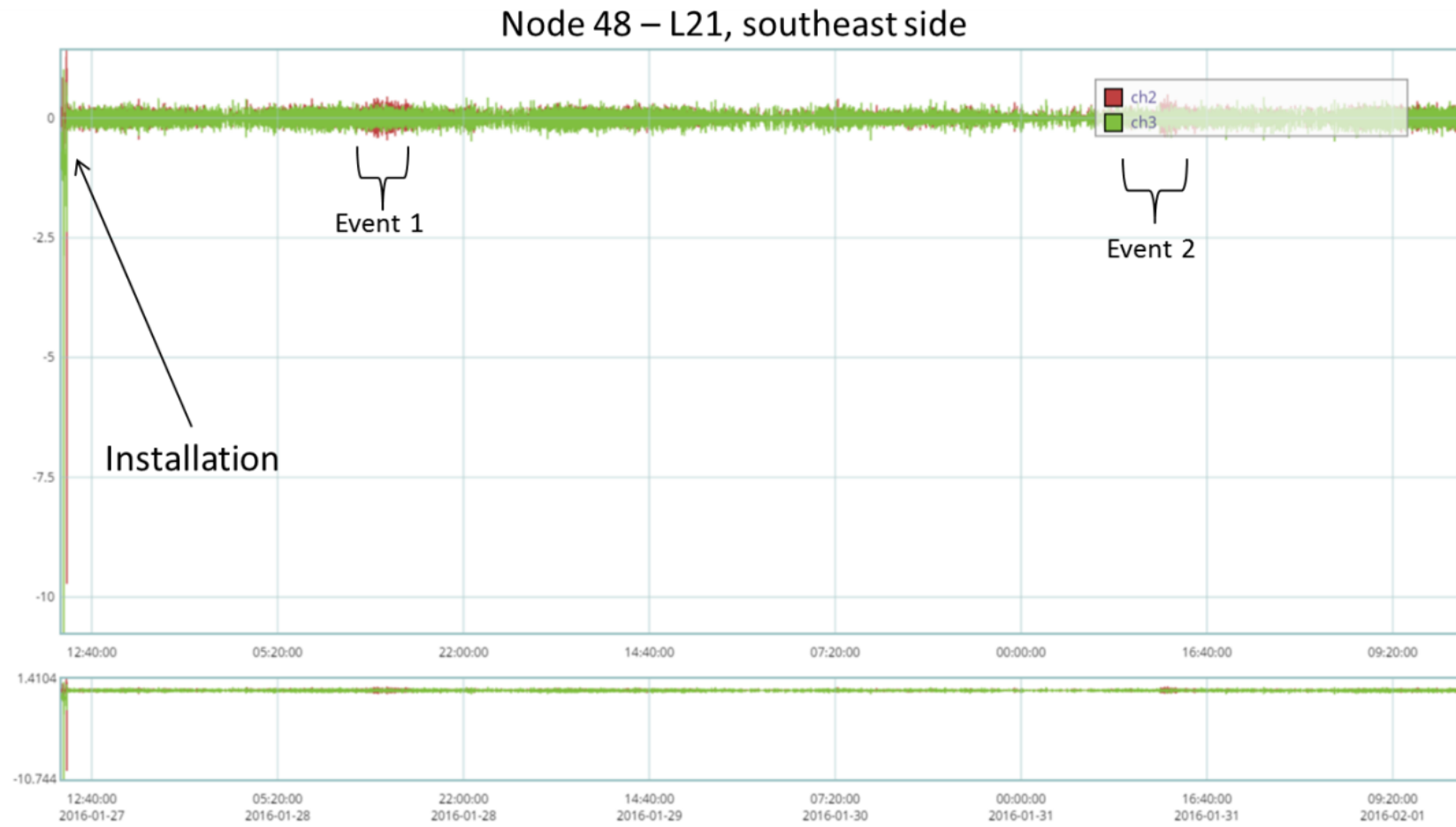


Figure 17. Data collected for Node 48 from January 27 to February 1, 2016

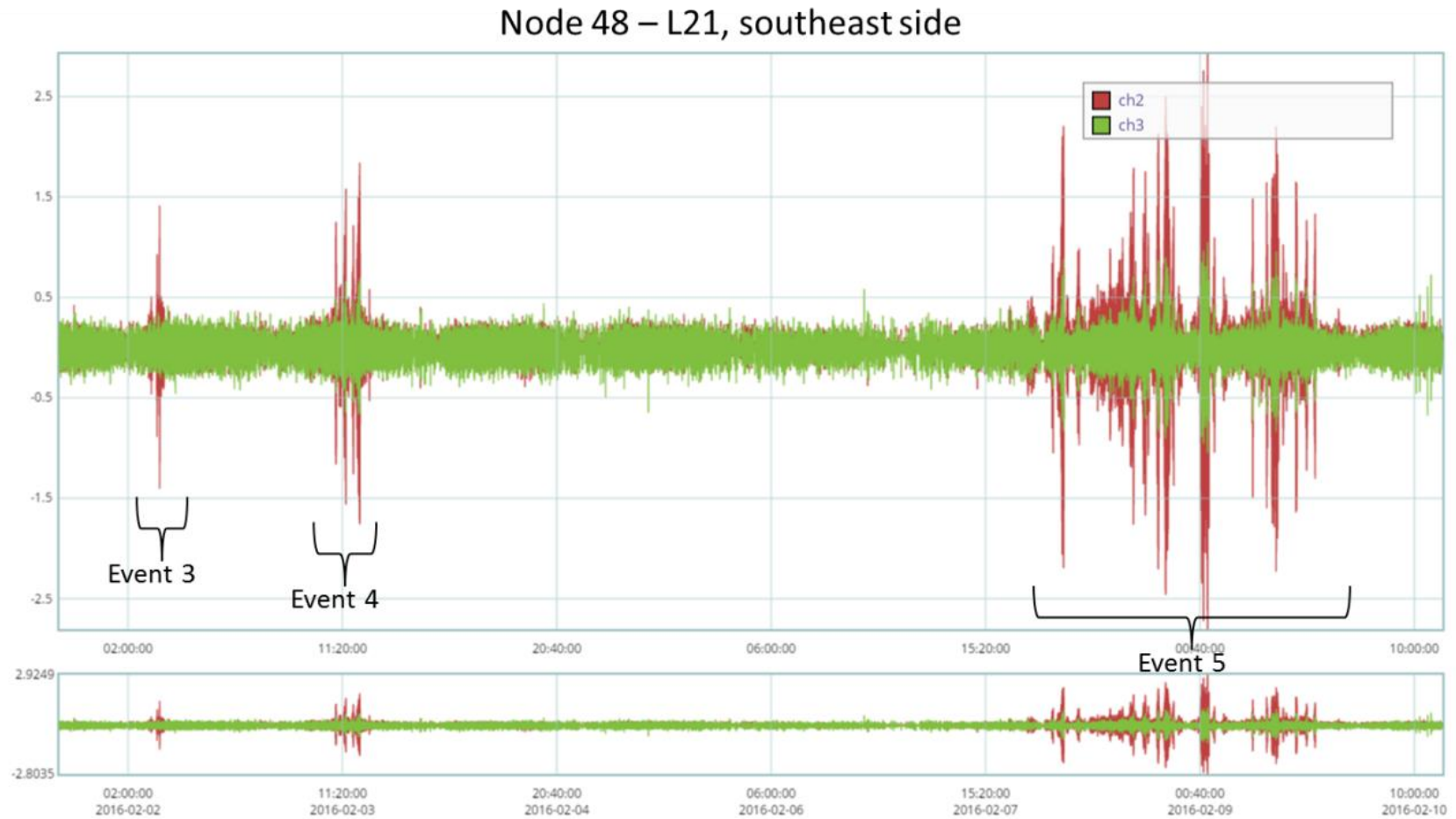


Figure 18. Data collected for Node 48 from February 1 to February 10, 2016

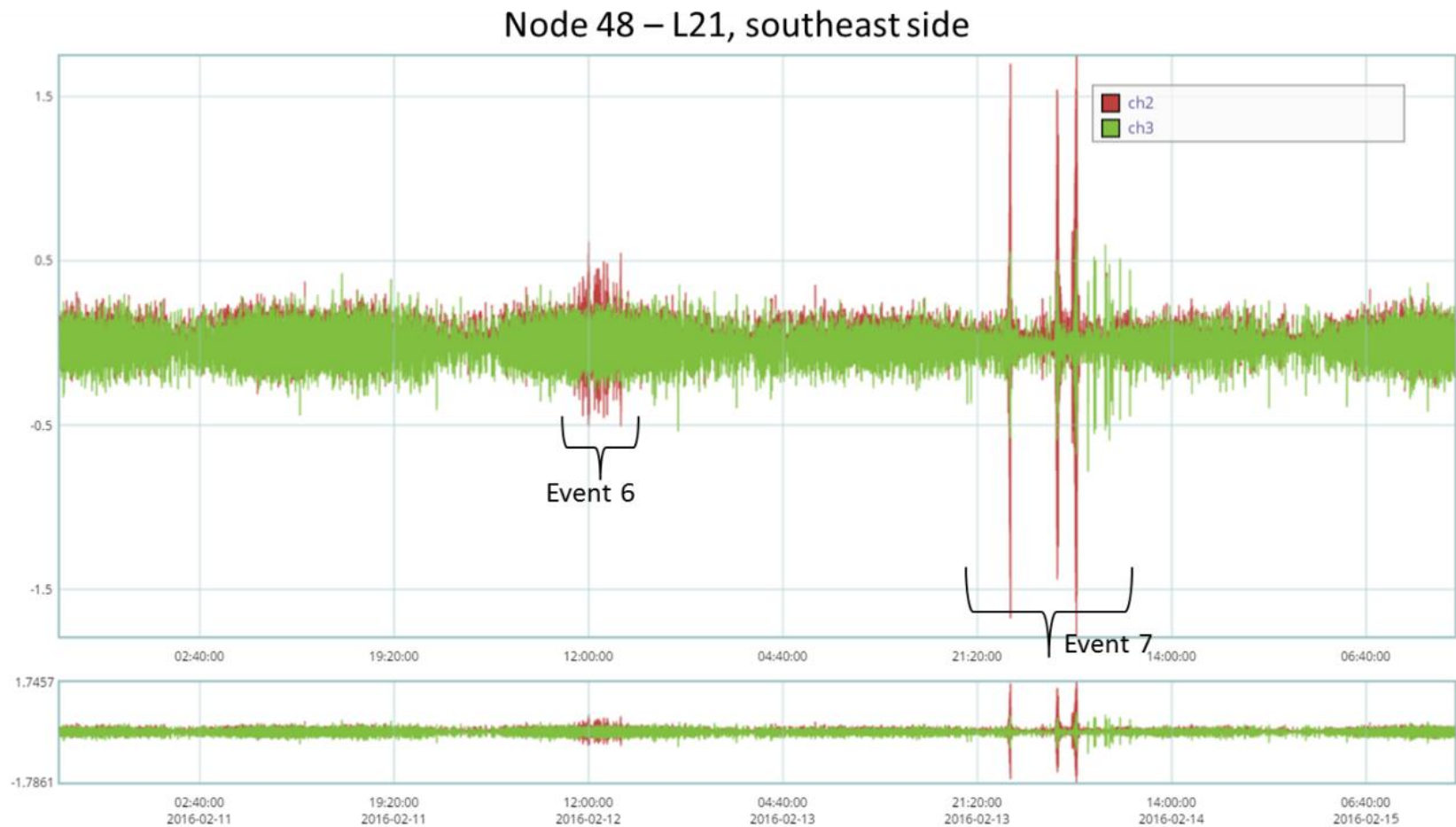


Figure 19. Data collected for Node 48 from February 10 to February 15, 2016

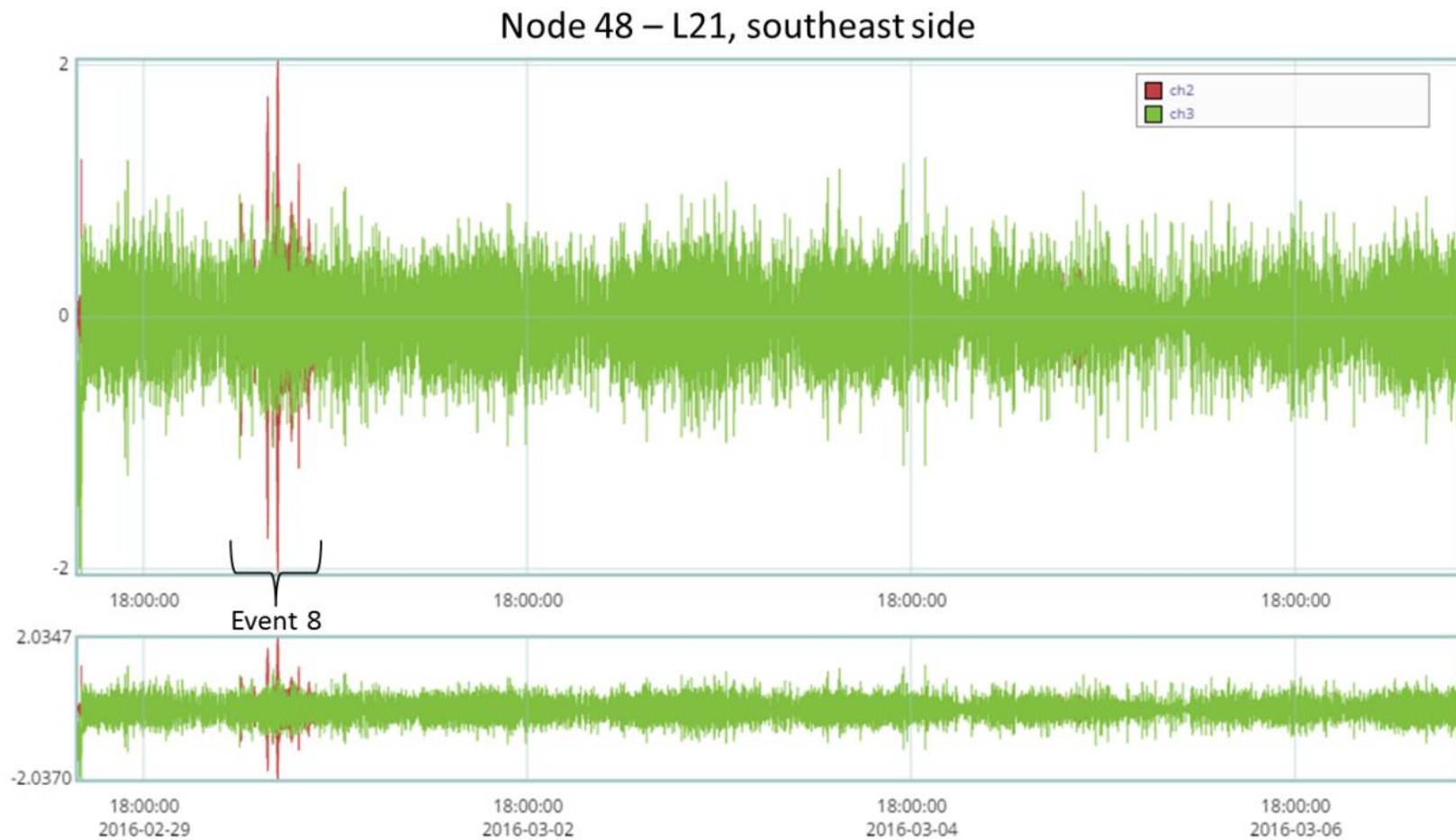


Figure 20. Data collected for Node 48 from February 29 to March 7, 2016

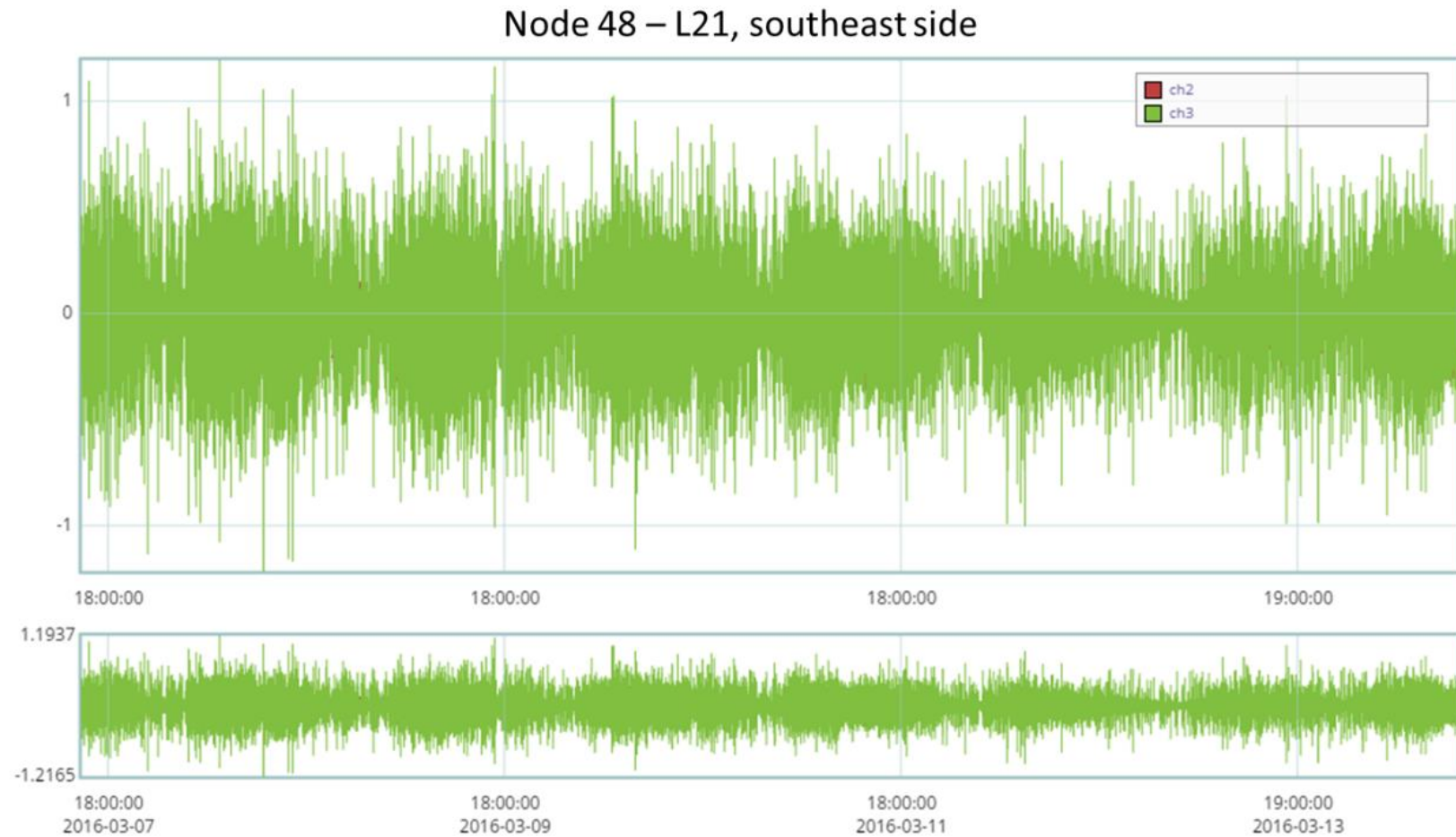


Figure 21. Data collected for Node 48 from March 7 to March 14, 2016

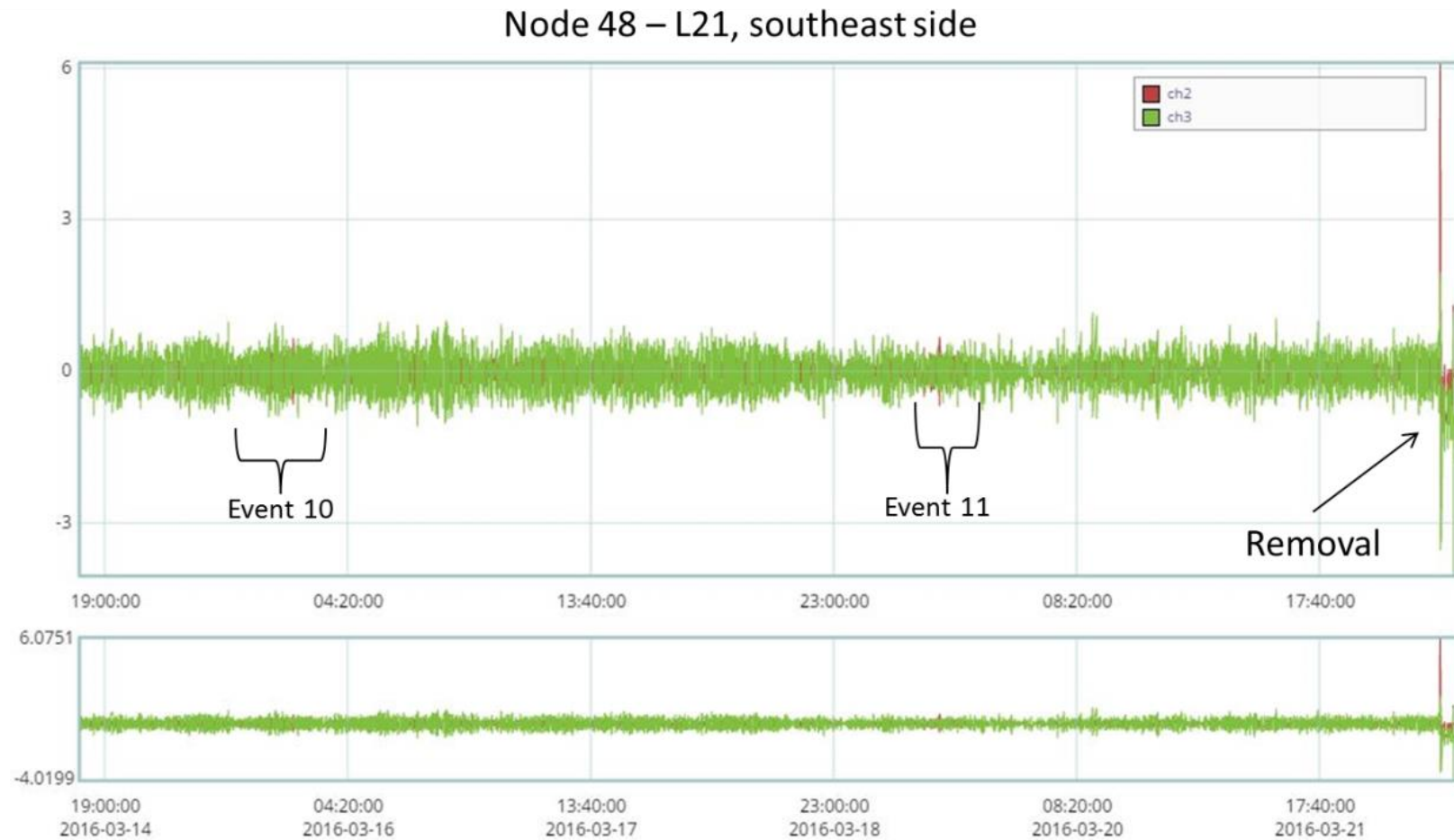


Figure 22. Data collected for Node 48 from March 14 to March 22, 2016

A.2 Node 49

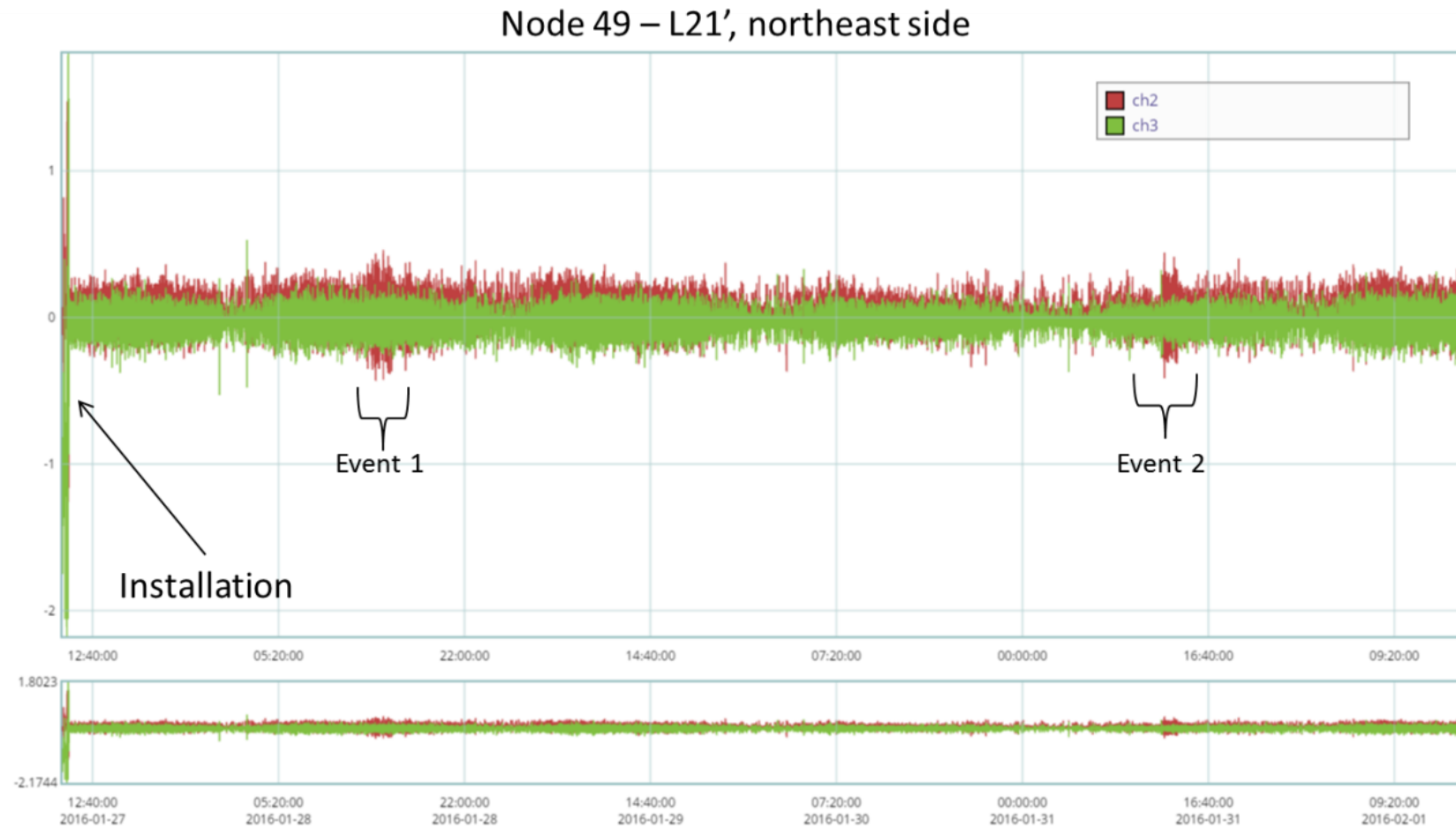


Figure 23. Data collected for Node 49 from January 27 to February 1, 2016

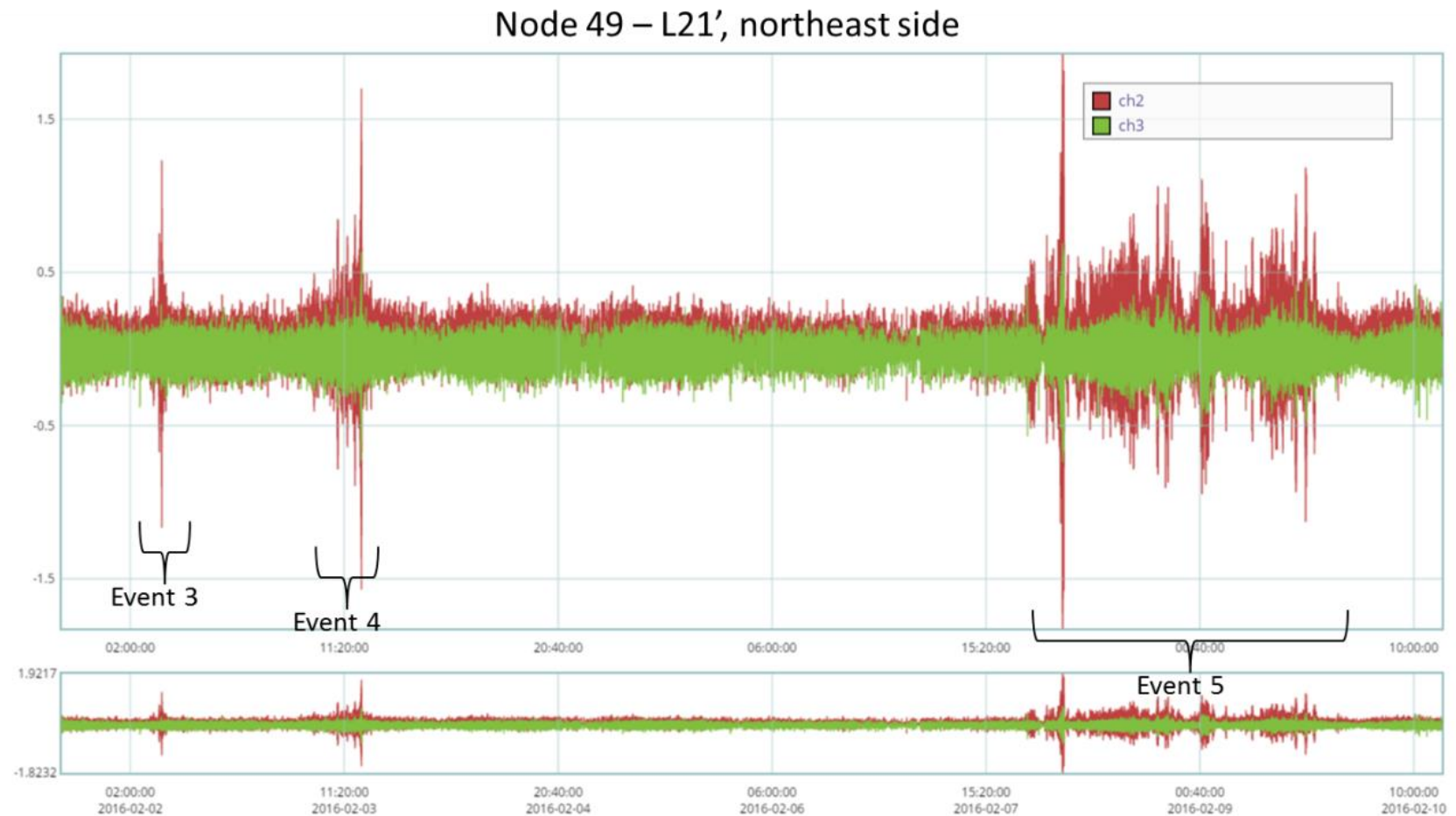


Figure 24. Data collected for Node 49 from February 1 to February 10, 2016

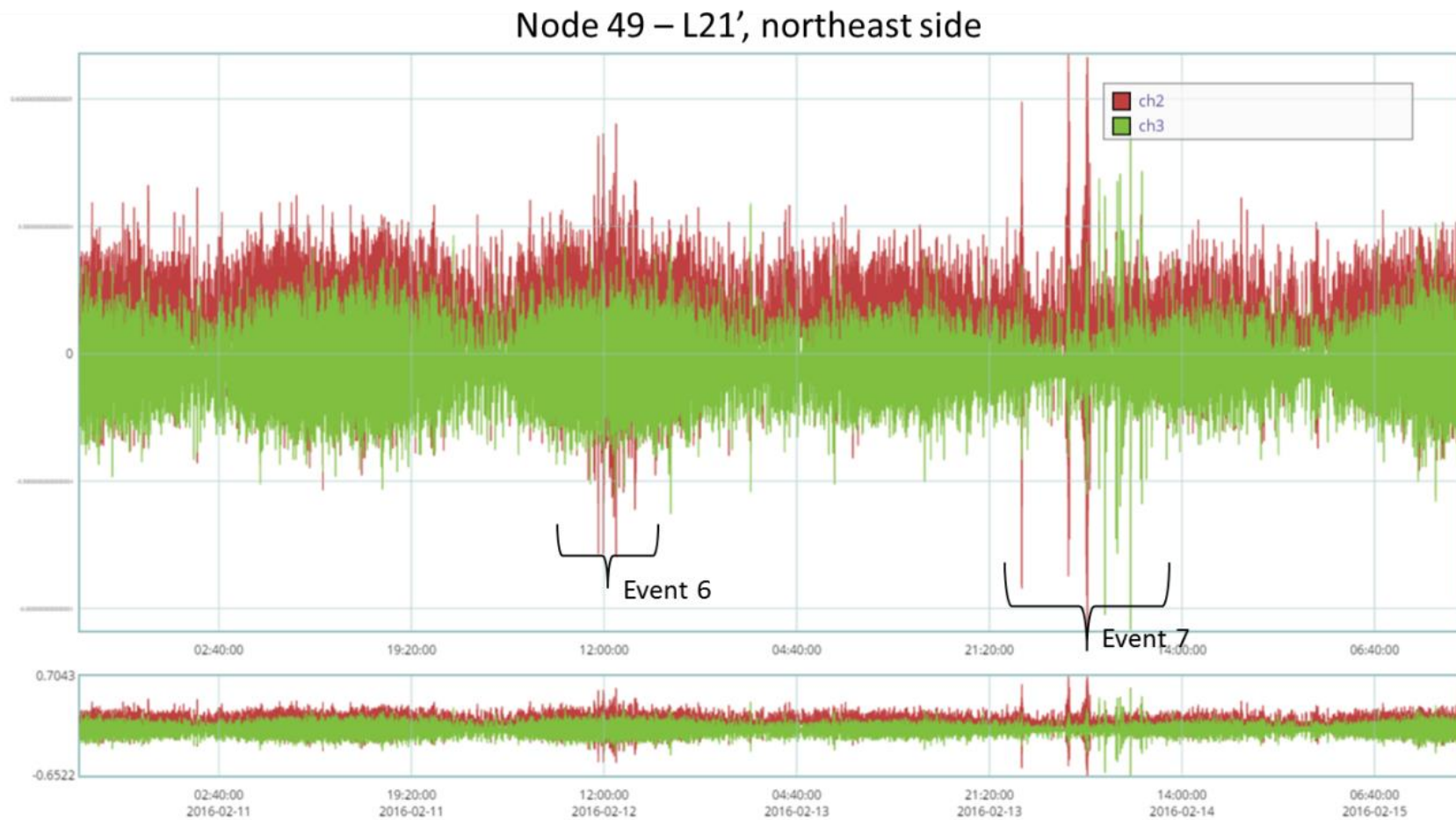


Figure 25. Data collected for Node 49 from February 10 to February 15, 2016

Node 49 – L21', northeast side

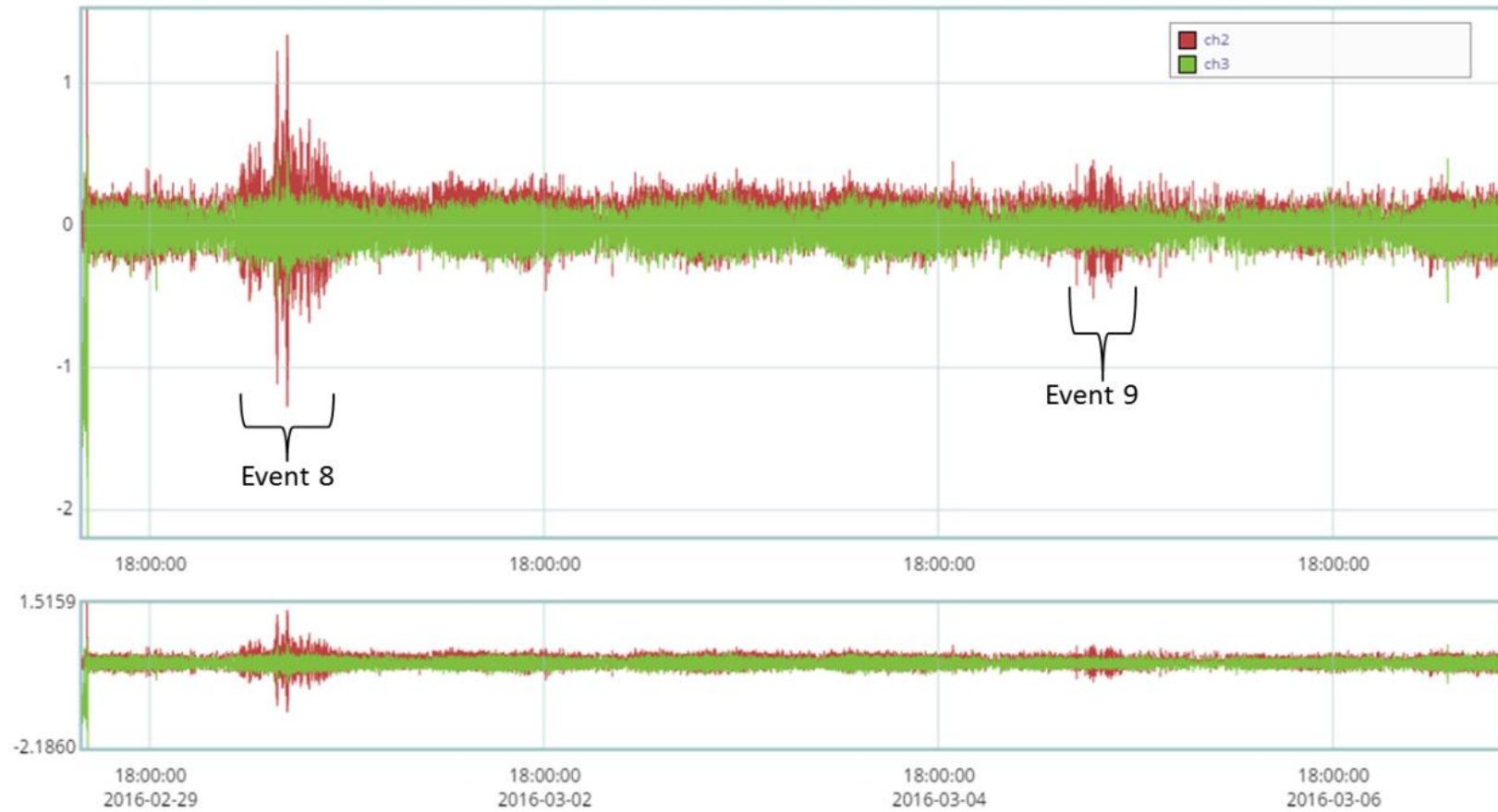


Figure 26. Data collected for Node 49 from February 29 to March 7, 2016

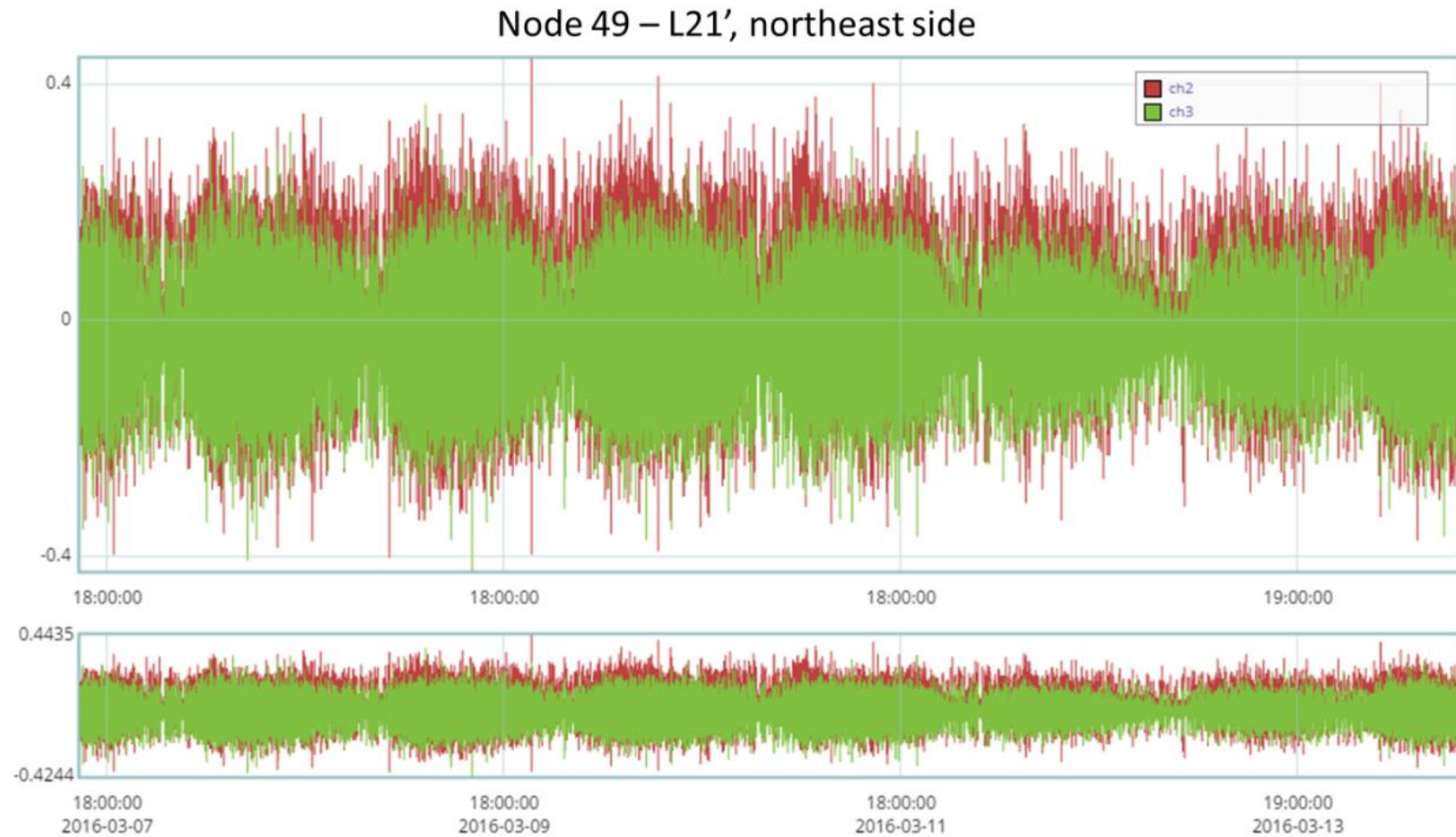


Figure 27. Data collected for Node 49 from March 7 to March 14, 2016

Node 49 – L21', northeast side



Figure 28. Data collected for Node 49 from March 14 to March 22, 2016

A.3 Node 50

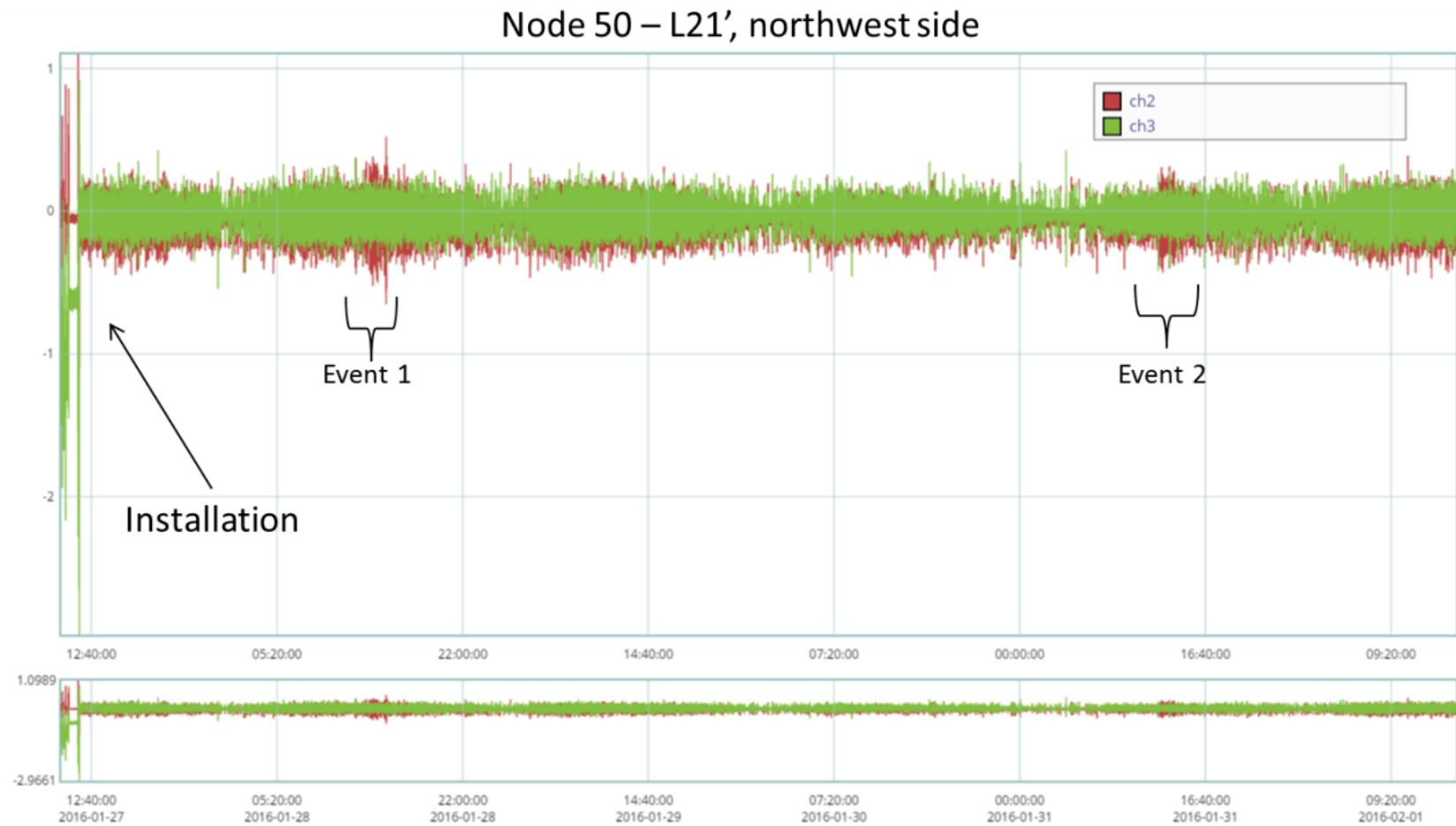


Figure 29. Data collected for Node 50 from January 27 to February 1, 2016

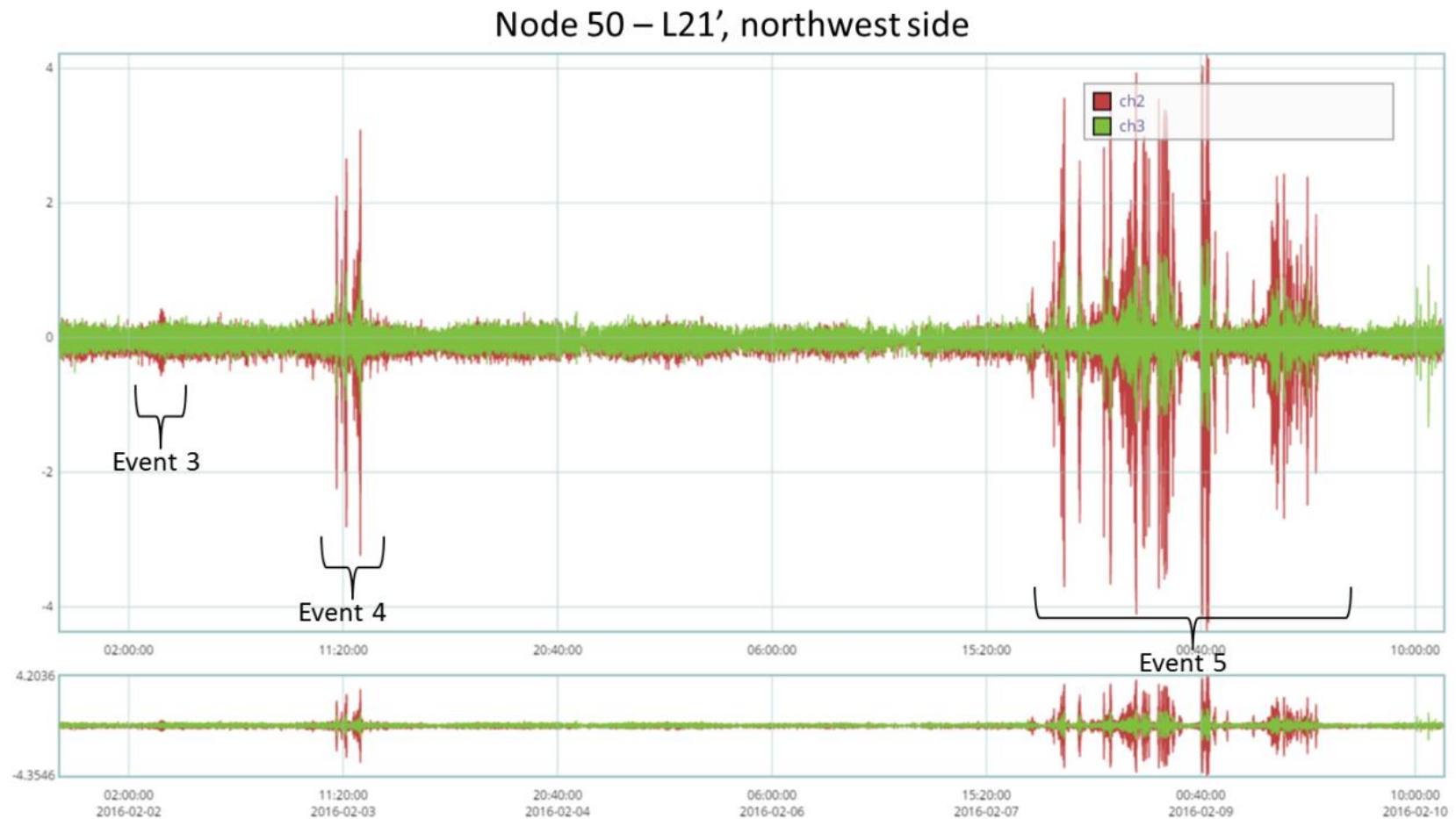


Figure 30. Data collected for Node 50 from February 1 to February 10, 2016

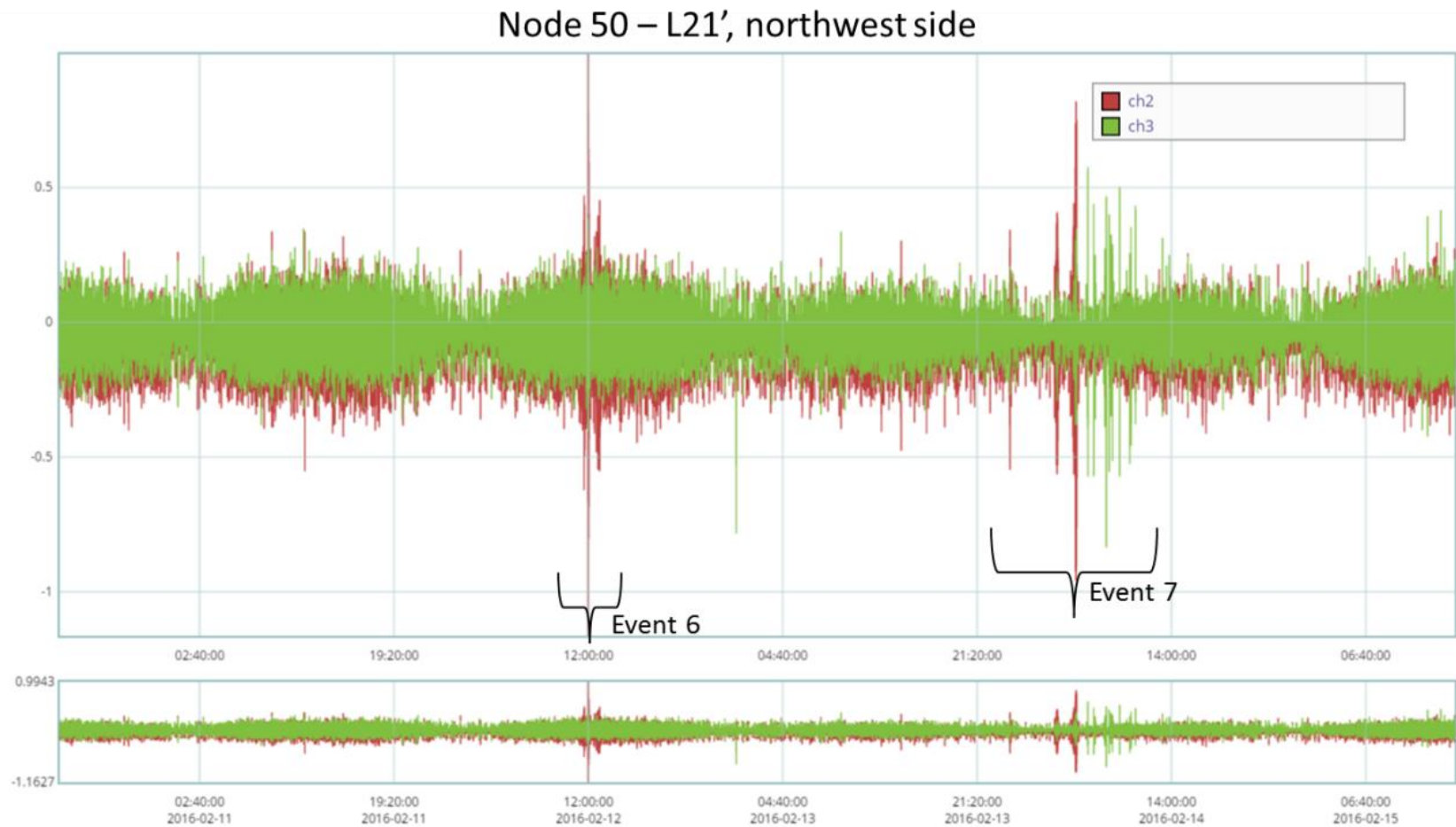


Figure 31. Data collected for Node 50 from February 10 to February 15, 2016

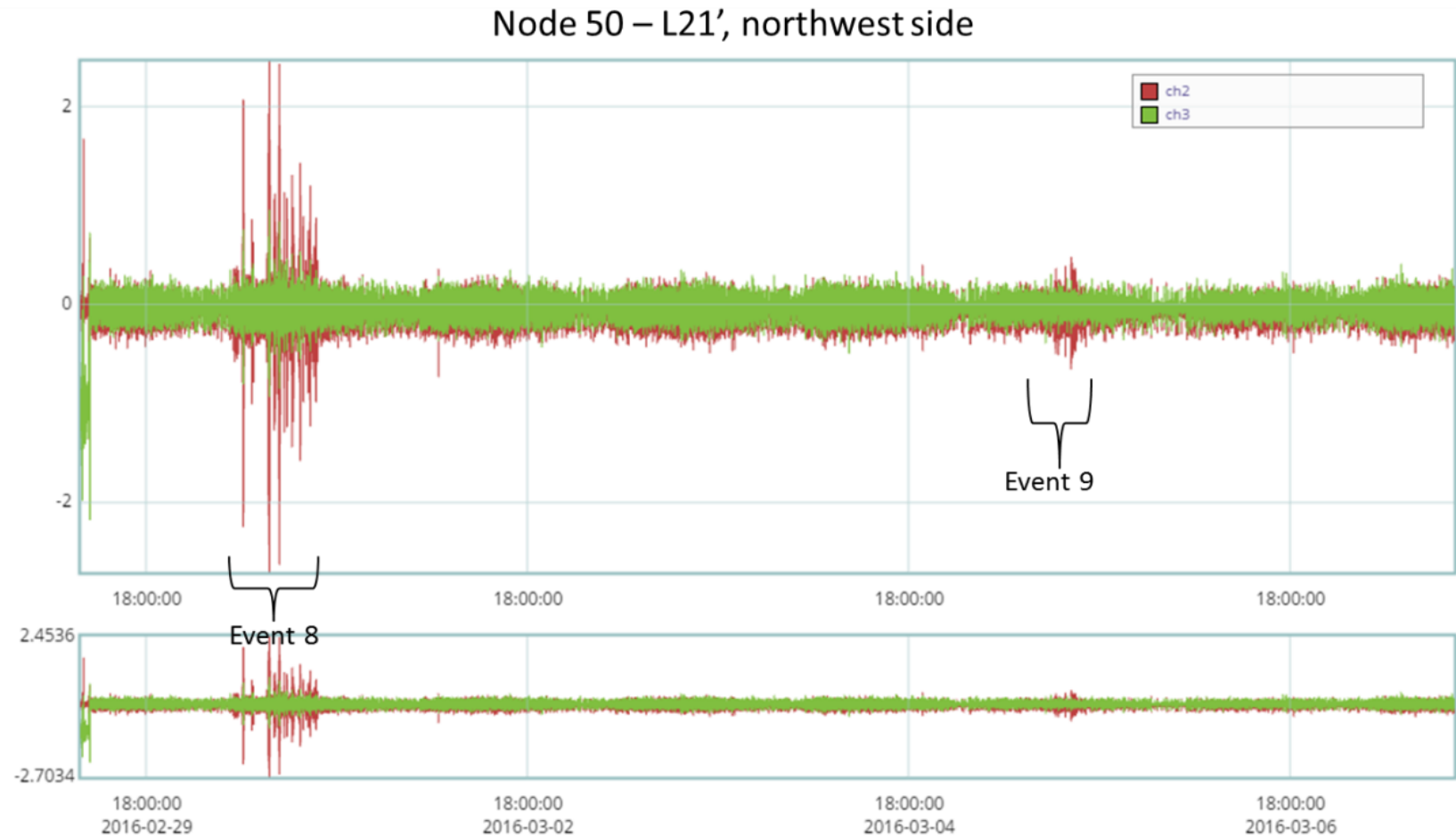


Figure 32. Data collected for Node 50 from February 29 to March 7, 2016

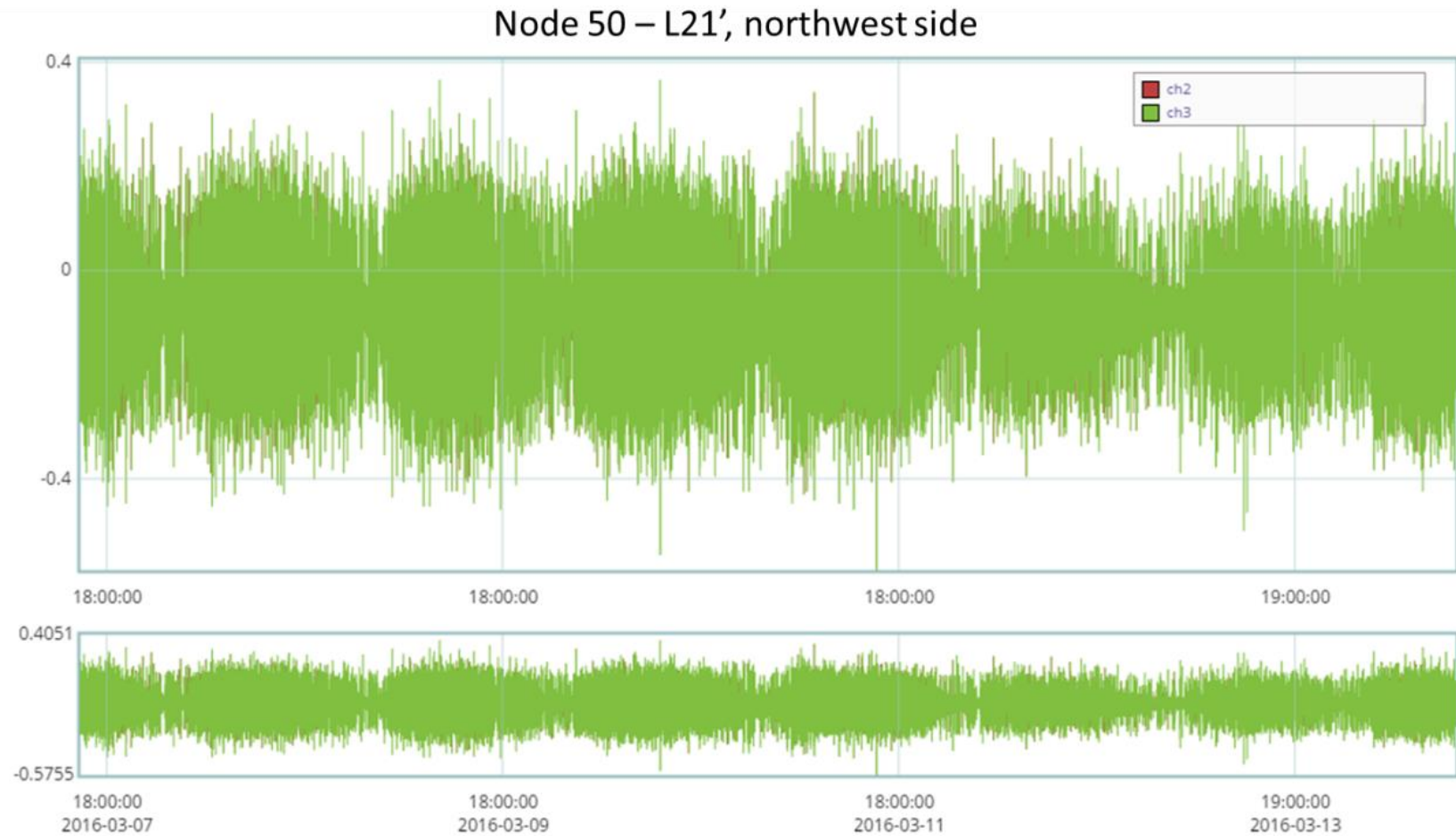


Figure 33. Data collected for Node 50 from March 7 to March 14, 2016

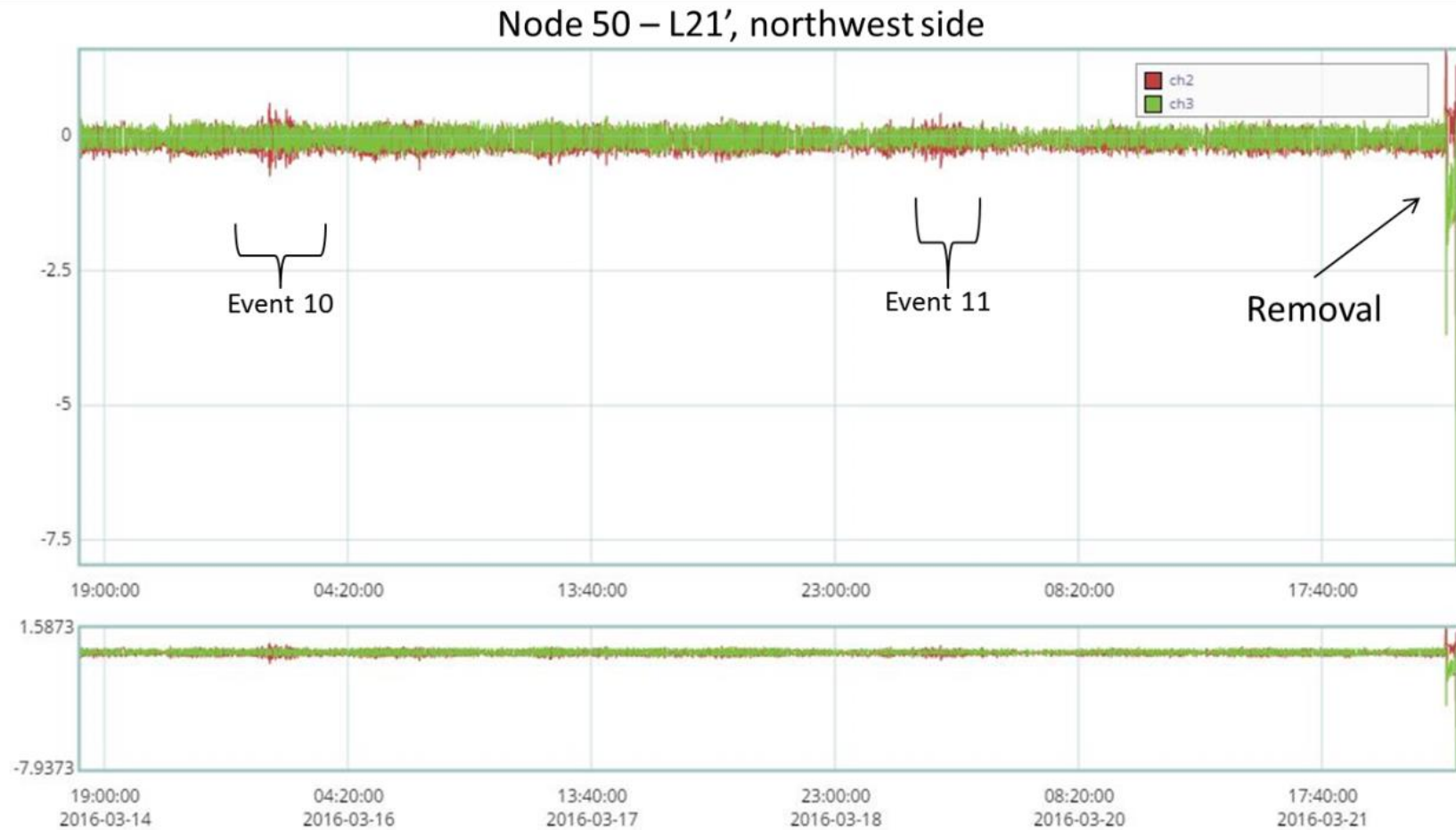


Figure 34. Data collected for Node 50 from March 14 to March 22, 2016

A.4 Node 51

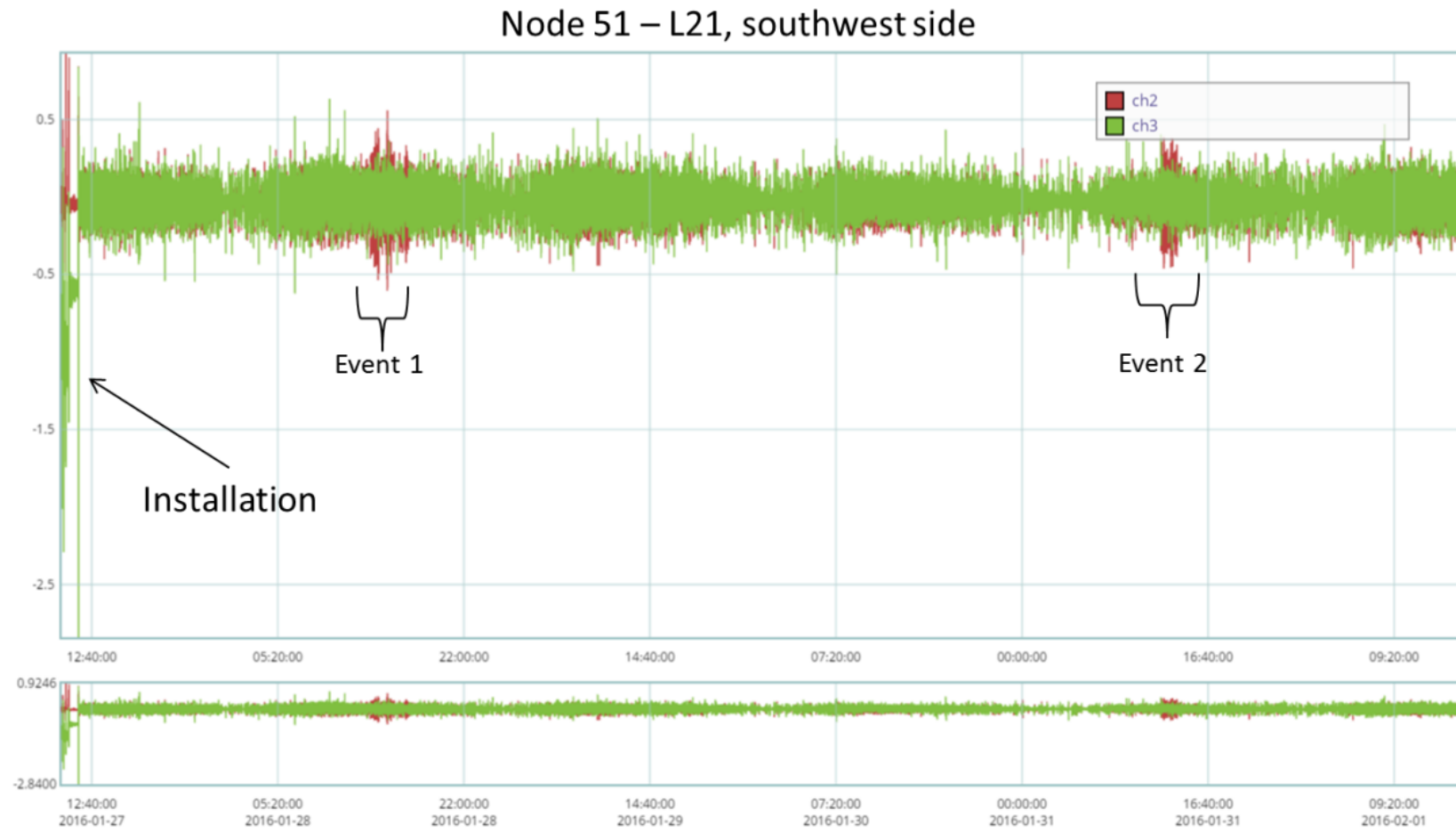


Figure 35. Data collected for Node 51 from January 27 to February 1, 2016

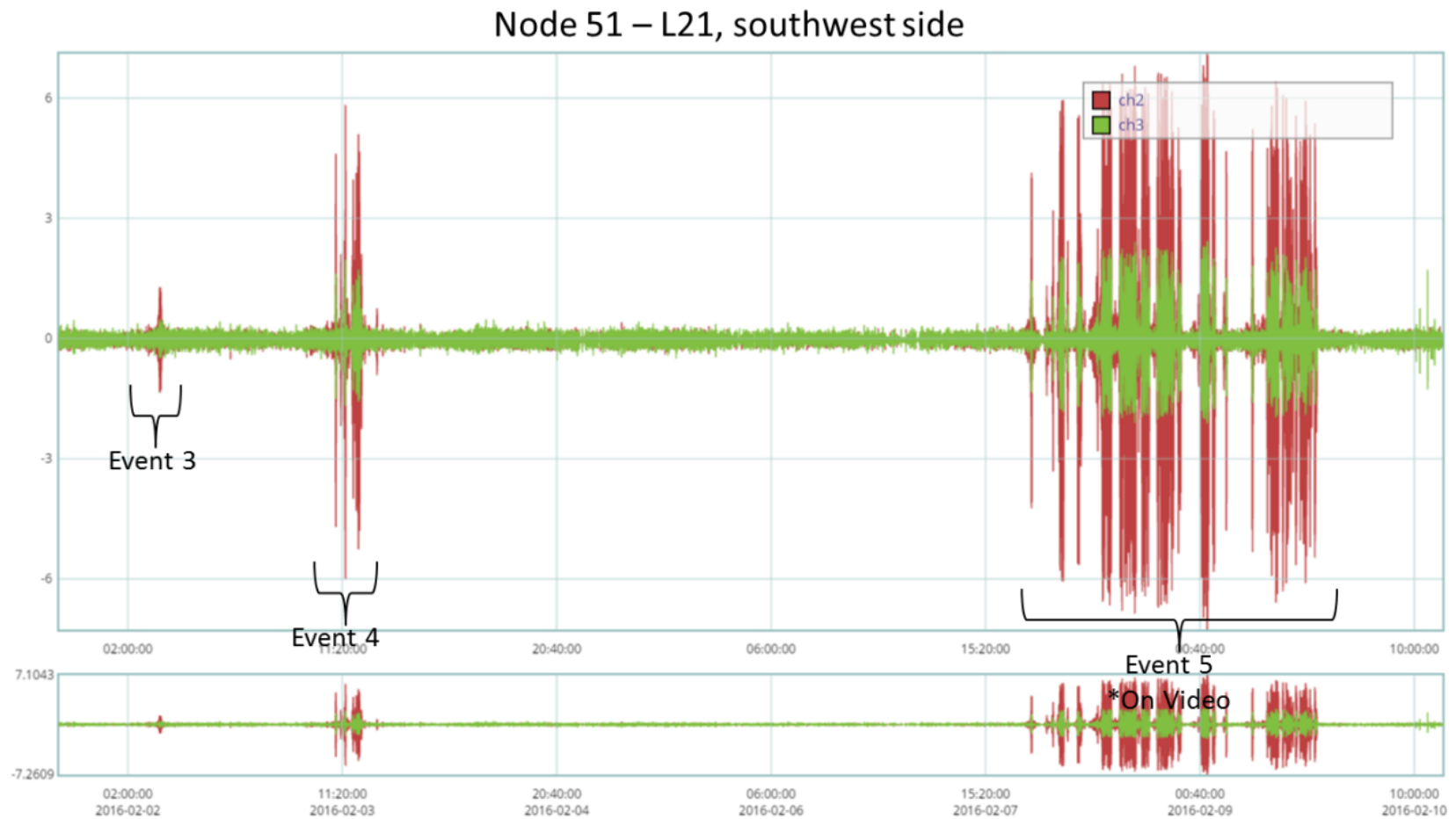


Figure 36. Data collected for Node 51 from February 1 to February 10, 2016

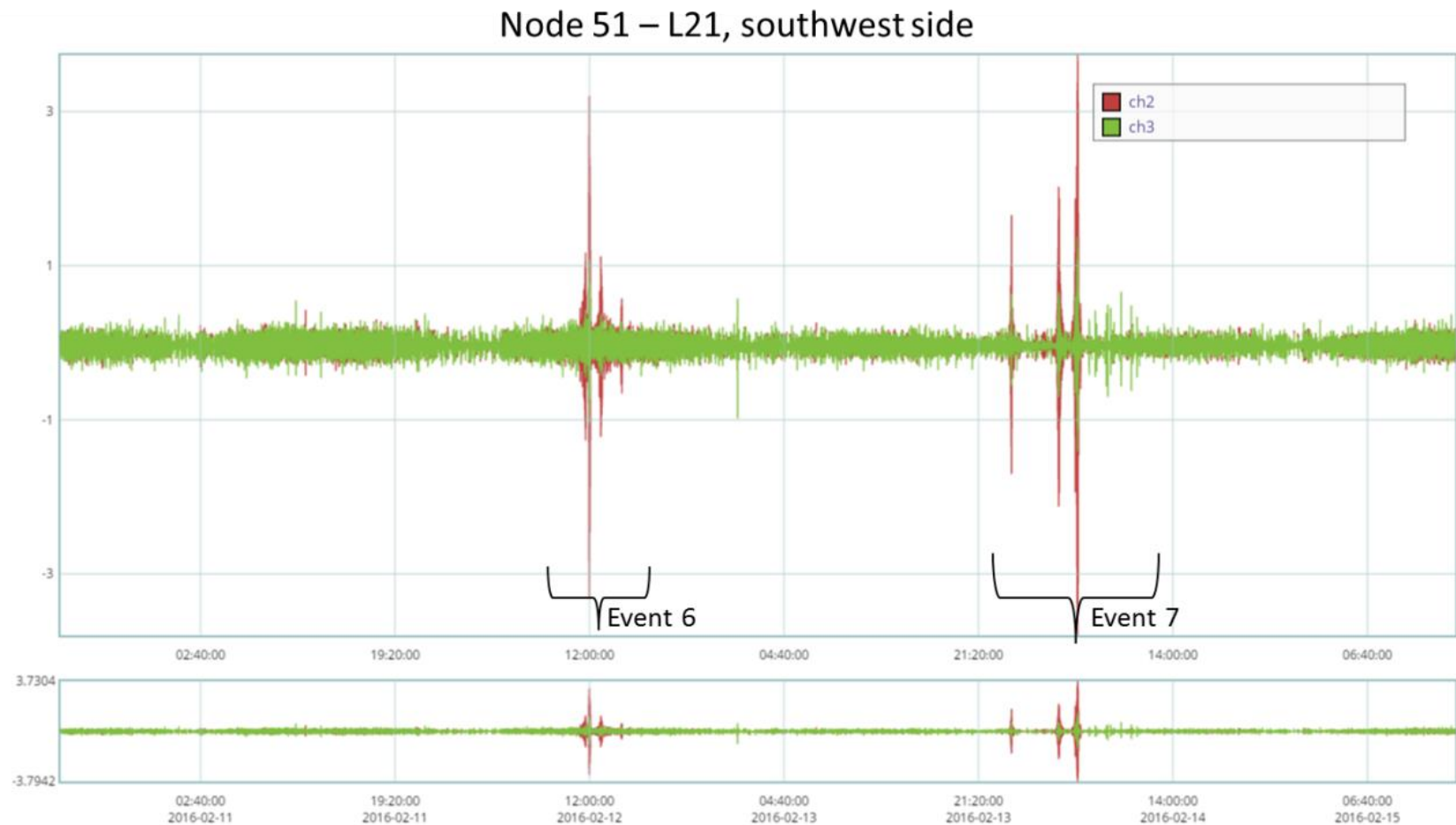


Figure 37. Data collected for Node 51 from February 10 to February 15, 2016

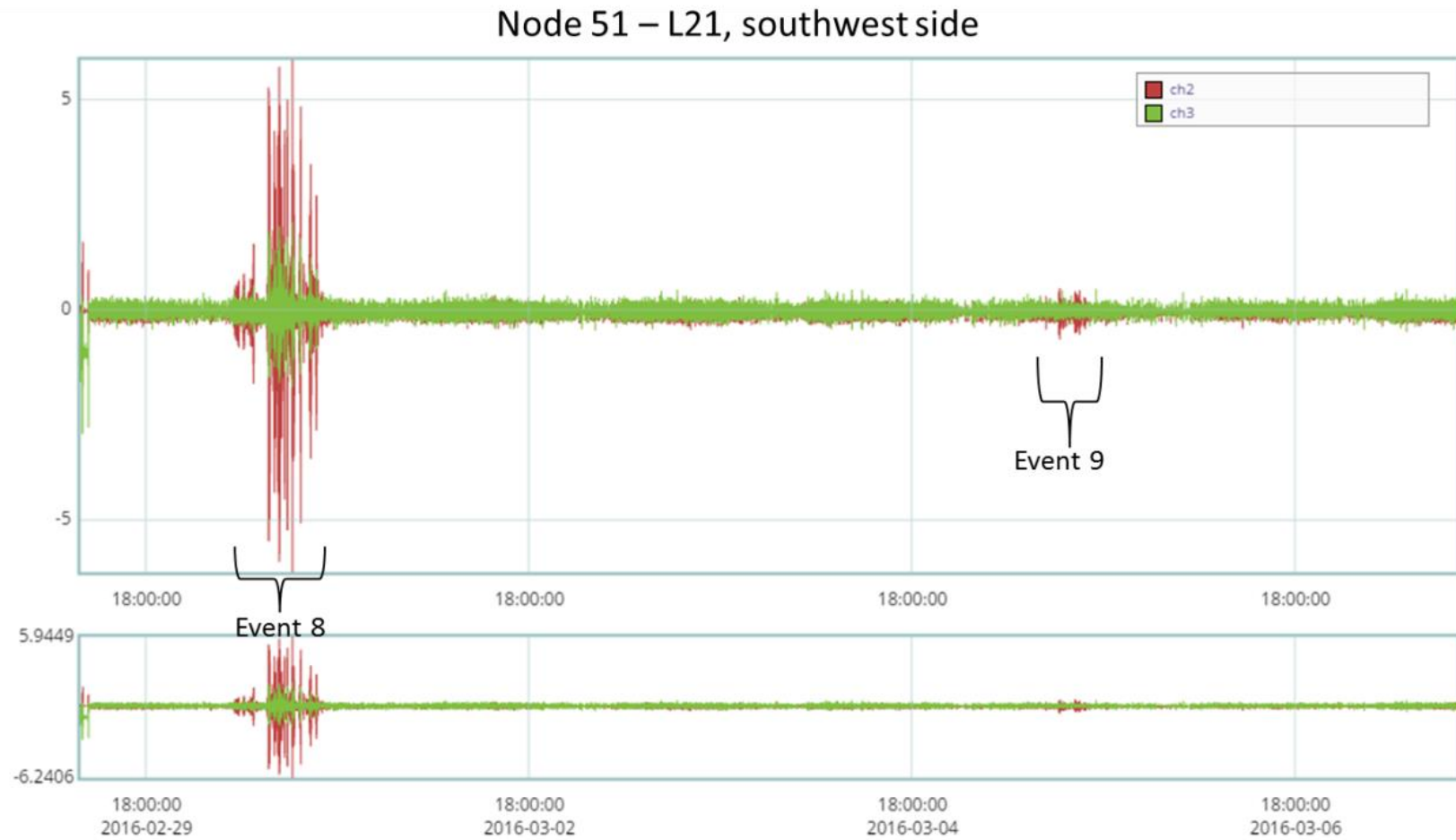


Figure 38. Data collected for Node 51 from February 29 to March 7, 2016

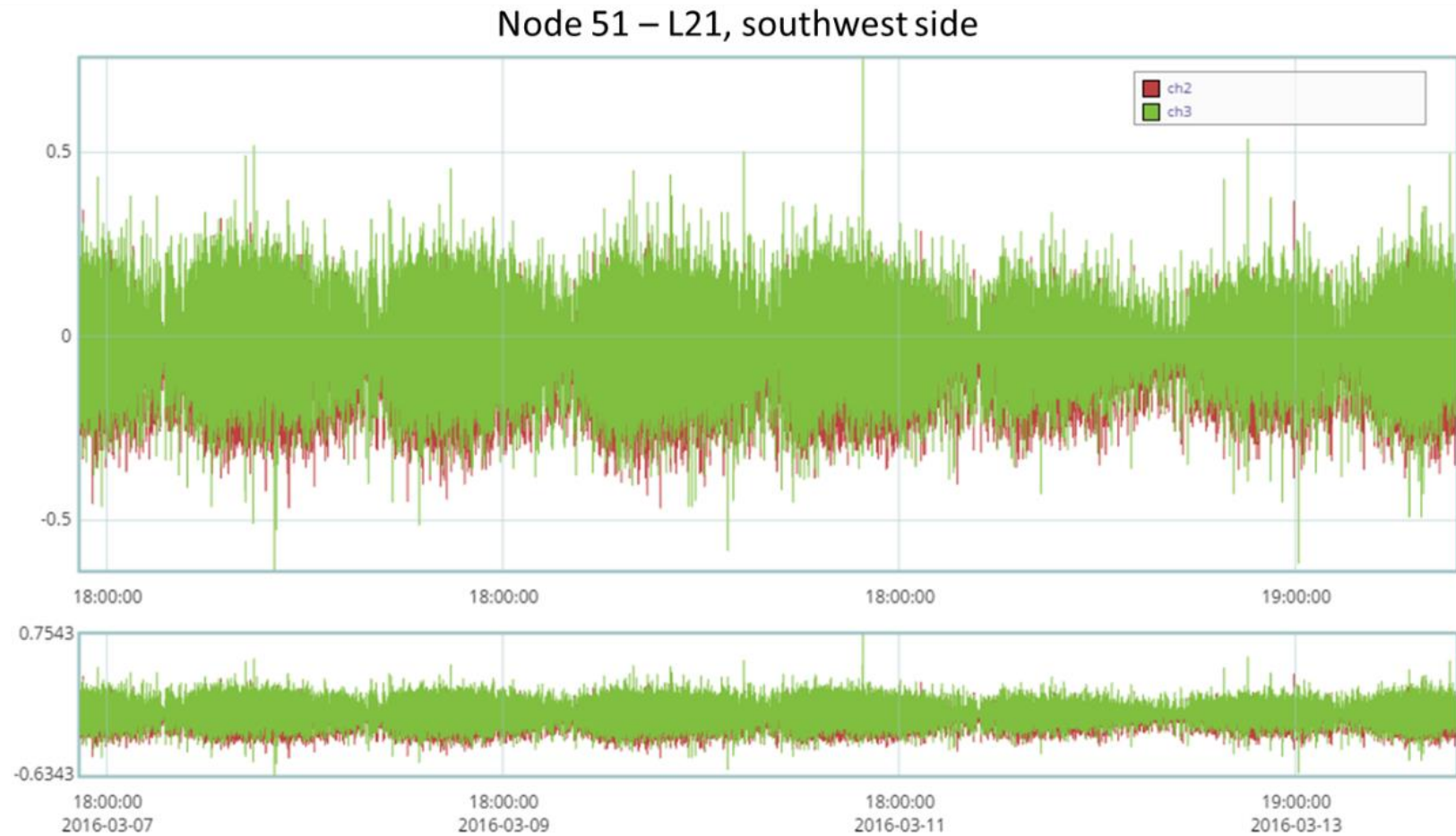


Figure 39. Data collected for Node 51 from March 7 to March 14, 2016

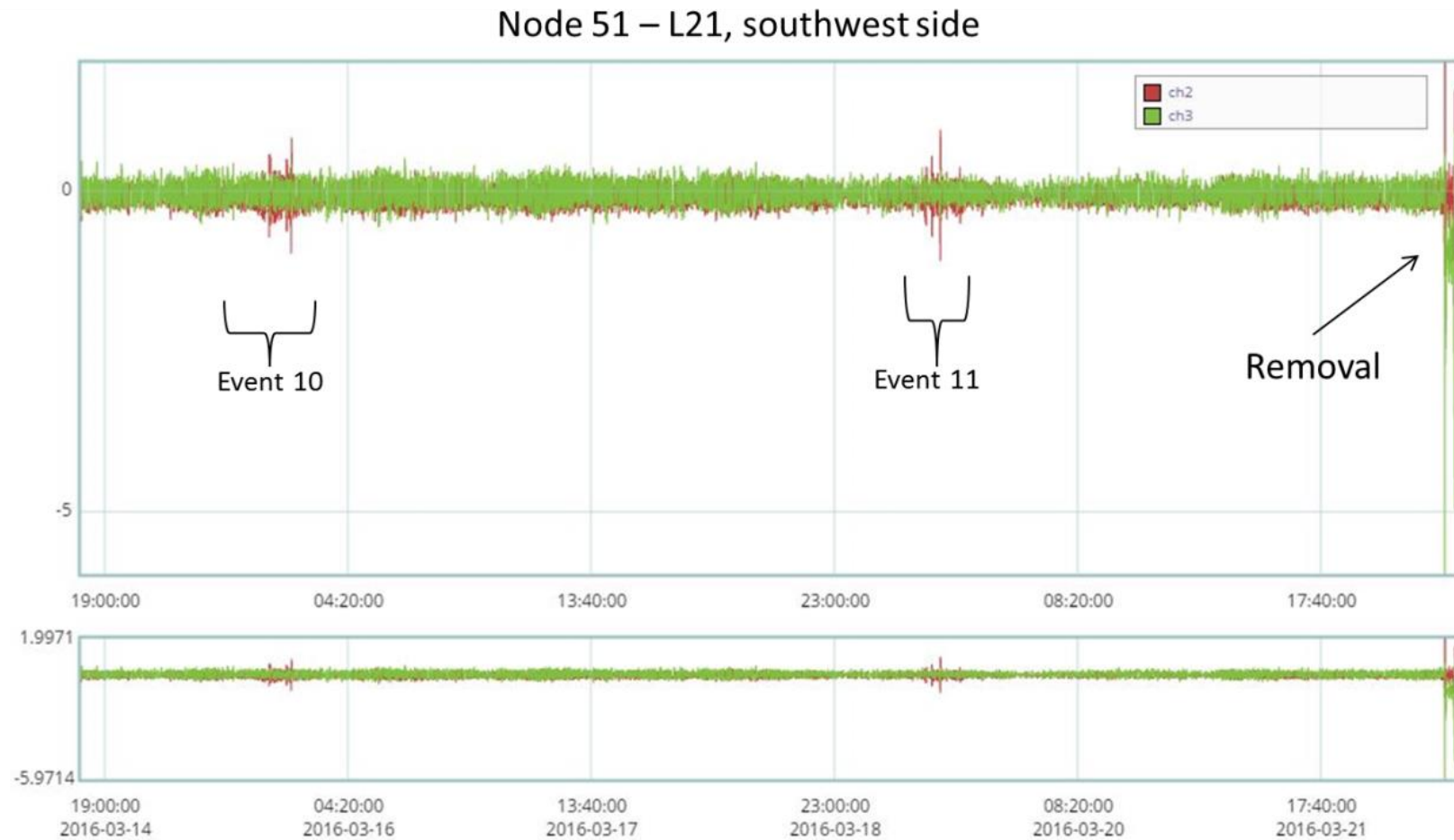


Figure 40. Data collected for Node 51 from March 14 to March 22, 2016